Year 4 Physics Performance task 2021

4RA Group 1, Problem 1

Contents Page

Class: 4RA

Names of Students: (A) Keith Chan Soong-Lin (4C - 3)

(B) Lau Ian Kai, Ethan (4C - 11)

(C) Tan Yu Jay (4C - 24)

(D) Bennetton Ang (4D - 5)

1 CONCEPT

The concept of our group's physics performance task is Mechanics.

2 OBJECTIVE

The objective of this project is to design and build a sail and keel for a given 3D-printed sailboat so that the sailboat can travel a distance of 30cm in the shortest possible time given a fixed wind direction, which is not known.

3 BACKGROUND READING

In considering the motion of a sailboat for this project, there are 2 main regions of interest: the sail-air interface and the keel-water interface.[1] In optimising the forces at the two interfaces mentioned above, we will need to consider *two key forces* — lift and drag, which are the forces defined as acting perpendicular and parallel to the wind/water direction (relative to the sail/keel respectively). Refer to the diagram to right for a diagram of the forces acting on a boat when wind is blown perpendicular to it.

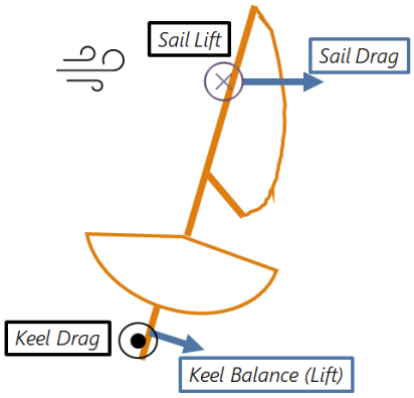

Sail-Air Interface

For the sail, the forces are primarily aerodynamic. The sail generates lift in perpendicular to airflow through a pressure differential between the front and back surfaces on the sail. For a fluid flow, we can use the *Streamline Curvature Theorem*. This can be stated as $\frac{\partial p}{\partial R} = \rho \frac{v^2}{R}$, where $\frac{\partial p}{\partial R}$ is the pressure differential perpendicular to fluid flow at each point along the flow (which is then summed up to get the total pressure on each side), ρ is the density, v is the velocity, and R is the radius of curvature of the airflow.

[1] As we are given a 3D-printed sailboat to optimise, any interactions on the hull-water interface (excluding the keel) is constant.

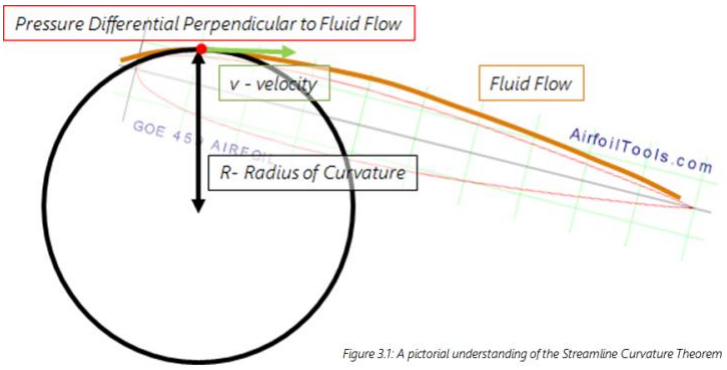

Figure 3.1: A pictorial understanding of the Streamline Curvature Theorem

Physically, this implies that there is a positive pressure gradient at a sail, and thus an outwards force radially from the curvature circle. As such, the angle at which the sail is tilted at, or the angle of attack (AoA), is of significance to the lift produced — the greater the angle, the greater the curvature of the airflow, and the greater the pressure differential. However, the fluid is only capable of "holding on" to the sharp curvature of the sail for so long — at higher angles of attack, the fluid flow becomes turbulent and detaches from the sail's curvature, resulting in a sudden loss of curvature and thus lift, which is known as *stalling*. Drag caused by pressure can be treated in a similar way. Unfortunately, analytical analysis of the flows is still being researched by current academia. As such, we turn to computational and empirical methods to find these values. (Computational methods and attempted flow visualisation can be found in Appendix D)

The Lift and Drag forces are calculated from their respective equations:

$$F_{lift} = \frac{1}{2} C_l \rho v^2 A$$

$$F_{Drag} = \frac{1}{2} C_D \rho v^2 A$$

Here, the C_l and C_D terms characterise the shape of the sail, including the AoA, and are treated above. Another major parameter that can affect both drag and lift is the reference area A, assumed as surface area in both cases. With a larger surface, both forces increase, and thus we expect more total force. Finally lift and drag can be turned into driving force (refer to Appendix A).

Keel-Water Interface

Keels serve two primary functions. A common problem with boats is their low moment of inertia, due to the height of the mast and low mass of the boat. After all, the moment of inertia can be roughly approximated to:

$$I = \frac{1}{2} m_{hull} {r_{hull}}^2 + \frac{1}{3} m_{mast} {L_{mast}}^2$$

This shows that the moment of inertia is extremely affected by the height of the mast. This makes the boat highly unstable, as very little force is required to exert a torque significant enough to

cause capsizing. Secondly, the keel is a hydrofoil, and helps to ensure that the boat travels in a straight line, particularly when the wind direction is not parallel to the direction of travel. This is done through similar principles outlined in the earlier section: when a sideways force is exerted on the boat, the keel turns with the boat, and as a result, a pressure differential and subsequently lift is created in the opposite direction of the side force. This effectively minimises sideways forces acting on the boat and ensures that the boat travels straight.

However, one should note that there are a variety of interactions that happen between the water just around the keel (boundary layer of the keel) and the keel itself, which inhibits the forward motion of the sailboat. For one, there is friction between the boundary layer and the keel, which can be approximated to the drag equation found above. Furthermore, at the end of the keel, the two boundary layers merge to form the wake at the trailing edge, which is extremely turbulent. This wake includes the formation of underwater vortices and eddies, which arise because friction of water against the sailboat results in rotational motion of water particles. These vortices and eddies not only result in a less efficient sailboat, but also hinders forward movement of the boat when such vortices create a small force backwards (due to the pressure differential).

4 DEVELOPMENT PROCESS OF THE PROTOTYPE

Given that this project requires us to investigate 2 parts of the sailboat (the sail and the keel), we decided to focus on two parameters of each part of the sailboat. For this project, a triangular sail was used to imitate the common genoa sails of many sailboats. As discussed in the background reading, the AoA affects the curvature of the airflow around the sail, and can create different forces for the same wind. In addition, the size of the sail can also affect the area of the sail, and change the thrust the boat receives. Hence, these two variables have to be investigated to optimise the sail-air interface. For the keel, we decided to focus on investigating the surface area of the keel, as well as the number of keels and the arrangement of such keels, because our literature has revealed to us that there are many different keel designs and number of keels, all of which work for different kinds of boats. Hence, we will need to investigate these variables to optimise the keel-water interface.

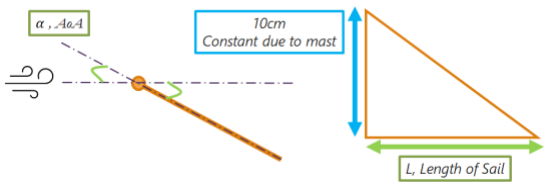

Fig 4.1: Schematic of Sail Variables and constants

The timeline for our project can be found in Table 4.1 below:

Time	**Event**
March Holidays	Extensive Review of literature, exploration and selection of variables
T2 Wk1-2	Design and Build Setups for testing, acquire materials needed
T2 Wk 3	Individual testing of variables
T2 Wk 4	Putting together and Evaluation
T2 Wk 5	Improvements, Additional Theory, and writing of report

Table 4.1: Work schedule for this project

Our dependent variables were the lift and drag forces for the sail, which allows us to get the driving force, as well as the drag of the keel, which we try to optimise. Then, in the evaluation phase, we rule out keels that allowed the boat to fall over, performing a "stability analysis" for the boat. We then select the keel with the lowest drag, that keeps the boat stable, and allows for the lowest time taken to move a distance of 30cm.

After our individual experiments (see Appendix), we reached the initial *prototype I* with the following dimensions:

Length of Sail	15cm
Optimal Angle of Attack	Variable, see appendix C
Length of Keel	3.00cm
Depth of Keel	1.00cm
Number of Keels	1
Distance between Keels (if any)	

Table 4.2: Specifications of Prototype I

5 TEST AND EVALUATE

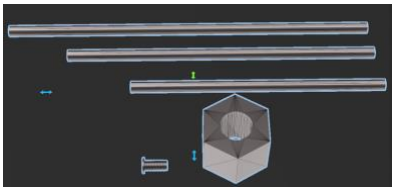

To develop our final prototype, we used the optimised design parameters above. Accuracy of cutting for the sail was controlled using a stencil, such as to ensure quality cutting, and new plastic folders were used to reduce the creases and imperfections in the plastic. To attach the appendages onto the boat, a small amount of hot glue was used for the keel on the bottom of the boat. For the sail, the following sail adjustment mechanism was designed, printed, and attached (details for how it works can be found in Appendix B).

The boat was then blown with a wind 45 degrees behind of it and recorded from the top. The timing to complete the 30cm distance was obtained from a video, similar to that of Ethan and Yu Jay's experiments (refer to Appendix C).

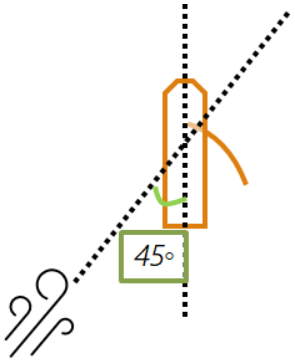

However, when we tested *Prototype I*, it could not withstand the wind and kept on rolling to the side and capsizing. (3/3 times tested) This was because our keel was too short, and its centre of mass and surface area were too low to stabilise the boat. Additionally, the sail was too long and hung over the boat, making it even more unstable. Given this, we had to resort to a different keel and sail, which would make the boat more stable. *Prototype II*, with a keel of length 9.00cm and depth 1.00cm, was also too unstable and was unable to stabilise the boat for most of our attempts. Hence, we turn to *Prototype III*, with the following specifications:

Length of Sail	10cm
Optimal Angle of Attack	Variable, see appendix Cw
Length of Keel	3.00cm
Depth of Keel	2.00cm
Number of Keels	1
Distance between Keels (if any)	

Table 5.1: Specifications of Prototype III

Prototype III was able to consistently sail stably, without capsizing. Hence, *Prototype III* was able to travel 30cm in the following timings, given a fixed wind from 45 degrees behind it:

Attempt	Prototype I timing/s	Capsized?	Prototype III timing/s	Capsized?
1	-	Yes	2.30	No
2	-	Yes	2.74	No
3	-	Yes	3.53	No

Table 5.2: Comparison of timings/lack thereof for prototypes I and III

Our final prototype was far more stable and was able to reliably complete the travel distance of 30cm 3/3 times in a relatively fast amount of time.

6 IMPROVEMENT AND REDESIGN ON THE FINAL PROTOTYPE

With *Prototype III* already producing desirable results, we wanted to further improve on the prototype. In order to achieve this, we tried varying the material of the sail. The materials we decided to try using were plastic (original material), canvas, and paper. The sails were cut according to the specifications of *Prototype III*, and the results can be found below:

Material of Sail	Time taken to travel 30cm/s			Average Timing/s
	Attempt 1	Attempt 2	Attempt 3	
Plastic (Original)	2.30	2.74	3.53	2.86
Paper	3.34	3.23	4.15	3.57
Canvas	3.72	-	4.15	3.94

Table 6.1: Timings of boat with different sail materials

An important factor in determining the effectiveness of a material as a sail is its porosity, or its ability to allow air to pass through it. If a material has high porosity (e.g. a sieve), much of the air would flow through the sail instead of going around it, and thus the force on the material is lower. As such, it is expected that canvas and paper, both slightly porous materials, are worse-off than plastic in providing a good driving force. Additionally, the canvas we used was thick (2mm) and heavy, which actually resulted in the boat capsizing once. The paper, being light and flimsy, constantly “flapped” in the wind, producing turbulent airflow and poor driving force, as well as a

lack of consistent timings. As such, we have confirmed that our original choice of material, plastic, was the best of them all, due to its light weight and minimal porosity.

In addition, we can further improve on *Prototype III* in the following ways:
Firstly, inducing a camber, or bend in the sail's airfoil would almost certainly increase the potential driving force, especially at small AoAs. Many ships make use of complex rigging systems and sail curvatures to induce a camber in the sail, which makes the sail curved. This increases the deflection of wind by the sail, allowing lift to be generated at a 0° AoA. Unfortunately, including a camber would change the entire shape of the Lift and Drag-AoA graphs. In the interest of time, we were unable to further investigate camber within this project.

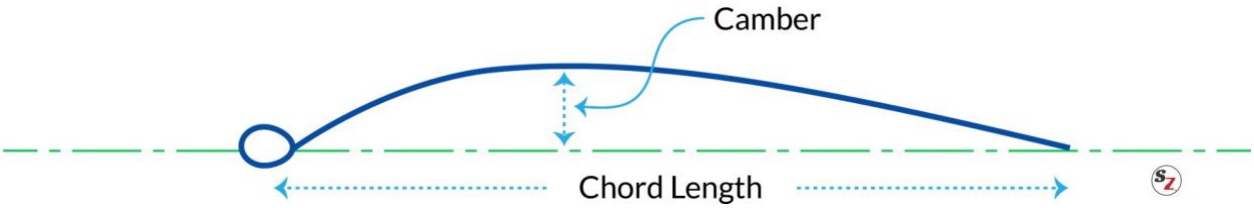

Figure 6.1: Pictorial representation of camber in a sail

In terms of improving our experiment, we believe that the steadiness of the wind source in the final testings could have been improved upon. This is as the hairdryer used was moved along with the boat by hand, which decreased its stability and thus the reliability of the results. We could improve on this by using a roller, such as those used in cupboards, to roll the hairdryer along with the boat, which would increase our reliability. Finally, whilst much care was taken to ensure that the design parameters were not affected by each other through our indirect testing, it is not necessarily the case that putting these optimised parameters together would lead to the best outcome.

7 REFERENCES

Babinsky, H. (2003). How do wings work? *Physics Education, 38* (6)*, 497–503.* https://doi.org/10.1088/0031-9120/38/6/001

NASA. (n.d.). Beginner's Guide to Aeronautics. Retrieved from https://www.grc.nasa.gov/www/k-12/airplane

Sloof, J.W. (2015). *The Aero- and Hydromechanics of Keel Yachts* (2nd Ed.). Springer.

Streamline Curvature and Lift Generation. (2007). Massachusetts Institute of Technology, retrieved from http://web.mit.edu/akiss/Public/streamlinecurvature.pdf

8 APPENDIX A: INDIRECT TESTING AS A CONTROL METHOD

Rationale

As the problem asks for us to minimise the time taken for the boat to travel 30cm, an obvious dependent variable would be just that. However, when trying to put this into practice, we run into an ensemble of problems.

Firstly, there is the lack of specificity over the wind source given — the task sheet explicitly states that the direction of wind and strength of wind is not known. Any understanding of sailing would tell us, therefore, that the orientation of the boat's sails should be changed depending on the wind direction given; an optimal sail configuration for wind blowing from the back would not be the same as that for wind blowing from the side.

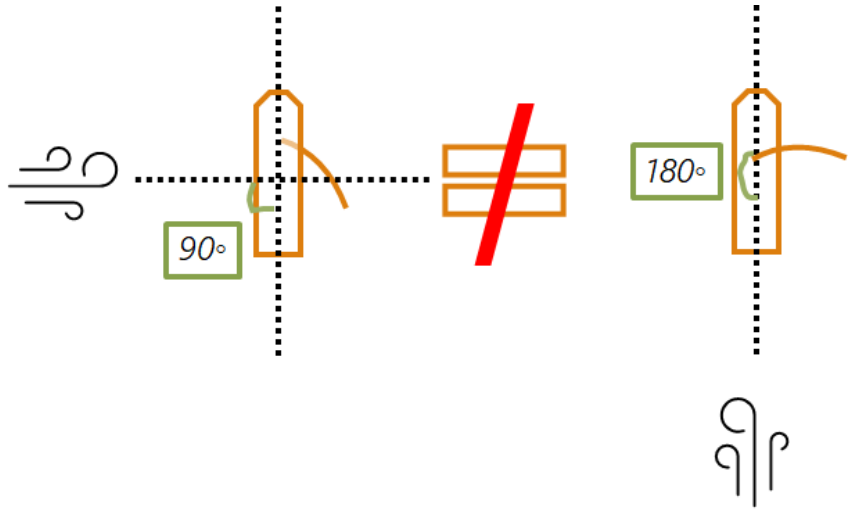

Figure 8.1: The optimal sail angle changes with the given wind angle

However, wind direction is not something that should be changed as a parameter, and varying it along with the angle of the sail and other parameters would be a long and tiresome process. (36 directions of wind × 36 angles of sail × 3 times each for accuracy = 3888 tests for angle of sail alone) Therefore a way must be found to adapt our boat to the wind conditions given, without having to manually test each wind angle ourselves. Indirect testing of the sails allows us to find the driving and side forces provided by the sail, given a wind angle, thus solving the problem of complexity at hand.

Secondly, control variables are much more difficult to maintain in an erratic basin of water, with strong wind blowing over it. Unsteady wave motion, induced waves from the wind, and reflection

of wind from the water surface are all uncontrollable factors that ruin the reliability of our results. We do not want errors and variances in the sail forces interfering with our results for the drag of the keel, and errors in the water surface interfering with our sail results. Thus, keeping these two components separate in individual testing is a good strategy.

Thirdly, even disregarding a plethora of possible experimental errors, and assuming a fixed wind direction coming from the side, complications arise with our original design for a combined experiment.

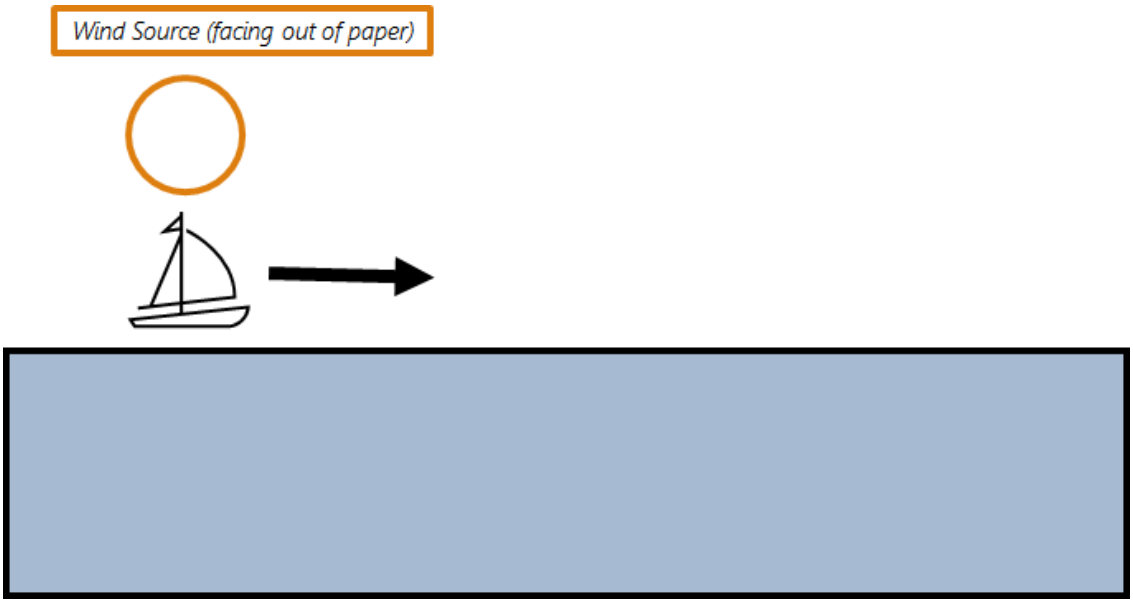

Figure 8.2: Schematic of original Experiment Design

The choice of wind source is a difficult one, with trade-offs no matter what — in testing, we had to choose between a large, but inconsistent and turbulent wind source like a fan, or a smaller, but more direct and laminar wind source like a hairdryer. Wind can be represented as a vector field of fluid flow, that changes at different points in the field. As such, the position of the boat from the wind source also has a large impact on the force experienced by the sail.

In the case of using the fan, due to the large size of the fan relative to the size of the boat, the boat only experiences a small section of the wind from the fan at any one point in time. However, a fan is not a uniform wind source — the wind is produced by large rotors that sweep wind outwards, and in discrete chunks from the fan, leading to an overall unevenness of wind, both in time and in position. In addition, most fans come with a “dead zone” in the centre, where no wind is blown, due to the placement of the motor there. As such, a fan, whilst a useful cooling device,

produces unevenness and error at a large scale as compared to the size of the boat, and is unsuitable for the project.

In the case of the hairdryer, we then face the issue of the dryer only blowing a narrow stream of wind. Whilst the hairdryer can blow air at a high velocity, and in a relatively even manner, it only does so for a small part of the movement of the sailboat:

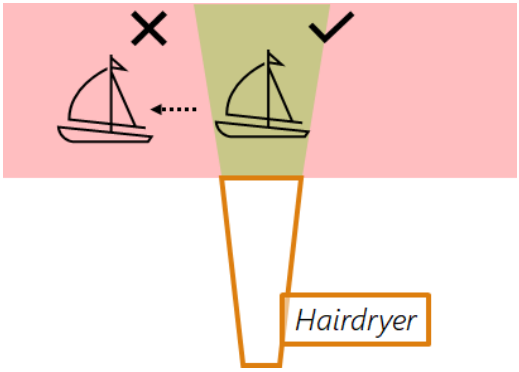

Figure 8.3: Diagram of the complications that arise from using a hairdryer as a wind source

In order for the hairdryer to be blowing the boat evenly throughout its entire motion, we would have to move the hairdryer along the water surface, without moving it up and down, at a changing velocity that is being measured. Therefore, we clearly see that this is not possible as well. In addition to the changing location of the boat, the movement of the boat poses a problem for us as well. Imagine you are travelling in a car, and you put your hand out a window:

Fig 8.4: A relative wind is felt by an object in its reference frame due to the movement of the object

As you can see, the movement of an object causes it to experience a relative wind opposite to its direction of travel. Similarly, the boat's movement causes a relative wind, which results in constant changes in the wind experienced by the boat. This is the reason it is theoretically more effective to travel at beam reach (90° to the wind direction) — when wind is blowing from behind, the boat

can only travel as fast as the wind, while the boat is able to travel significantly faster than the wind at beam reach because the relative wind does not affect the motion as much.

In our theoretical treatment of this, we assume the effect of relative wind to be negligible due to the high wind speed used, and relatively lower speed of the boat. However, we still need to mitigate the inaccuracies caused by this effect in testing. Therefore, indirect testing allows us to keep the boat that is being tested in one place, such that consistent wind may be blown onto it and measured, and the problems of relative wind may be removed. Finally, for the sail, attaching and removing the sail from the mast is difficult to do accurately. Indirect testing allows us to do tests without the boat, and thus have multiple sails lined up and adjusted, as well as to do concurrent tests of the sail and the keel, saving valuable time.

Design of Indirect Testing Methods

For the sails, a home-made wind tunnel was used. Steady wind is blown towards the sail, inducing both a lift and drag. These forces are split apart by perpendicular levers, and thus we can measure them separately; by splitting the total aerodynamic force into orthogonal components, we can manipulate and combine them as we wish to find the force given any wind direction. In this way, the measurement of the forces on the sail can be thought of as measuring a vector to the orthogonal basis of the lift and drag components. Details on the construction of said wind tunnel can be found in Appendix B**.** For the keel, in order to reduce the effects of wind force variances, a string was instead used to pull the boat forward in the water. Similarly, details can be found in Appendix B**.**

Significance of Results obtained from Indirect Testing Methods

As the name suggests, indirect testing methods are *indirect*, and thus the data collected must be processed in order to be made sense of. For the case of the keel, the processing is simple — we want to find a keel that can produce the least drag, whilst still keeping the boat stable. Hence, stability and travel times were measured and plotted.

For the case of the sail, the process is more complicated. The point of indirect testing is to get around the lack of specificity regarding the given wind direction. Therefore, in order to link our results back to the original problem, we need to invoke vector addition to find the driving force (the force that moves the boat in the forward direction) and the side force (the one perpendicular to the driving force). Essentially, we are adding the lift and drag force vectors (which are

orthogonal) together, and then renormalising them to the frame of reference of the boat, performing a change in coordinate system through a rotation of angle β.

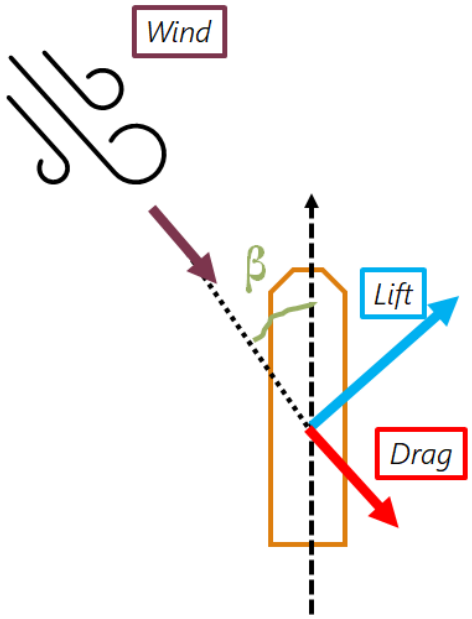

Figure 8.4: Vector diagram of forces acting on a sailboat due to the sail

From the diagram, we can get the driving force as:

$$T = L\sin\beta - D\cos\beta = L(\sin\beta - \frac{D}{L}\cos\beta)$$

Therefore, we want to be able to provide a maximum T for any given wind angle. Since $\sin\beta$ and $\cos\beta$ are constants, this value is maximised for:

$$\frac{dL}{d\alpha}\sin\beta - \frac{dD}{d\alpha}\cos\beta = 0$$

Which can be further simplified into:

$$\frac{dD}{dL} = \tan\beta$$

This can be computationally differentiated and solved to get the angle of attack α that satisfies this condition. Therefore, we can use this to choose our AoA when given any wind direction. The treatment and visualisation of this is found in Appendix C (Section 10.1), where we undergo experimental design and testing of the AoA.

9 APPENDIX B: EXPERIMENTAL APPARATUS

As all of the experiments were carried out in a home-lab and school-setting, without access to high-end measurement and securing devices, many of our apparatus had to be creatively put together, so as to fit within the confines of what we had readily accessible to us, and within the limit of our $50 budget. Thus, many of the materials used were scrap materials like cardboard, and the rest were common household items. Of the $50 budget allocated to us, we spent $0.

In this part of the appendix, we will describe the process of designing each of the apparatus used, and our thought process for designing the experiment the way we did, with the materials we used. Whilst not listed as a part of the experimental procedure, it represents the work done in acquiring the materials and improvising the specialised apparatus used in the experiment — It is prior work for preparation of the experimental procedure and is thus described as such.

Wind Tunnel

In order to measure values of lift and drag from a sail, a wind tunnel is designed. Here is a schematic of the wind tunnel, prior to construction:

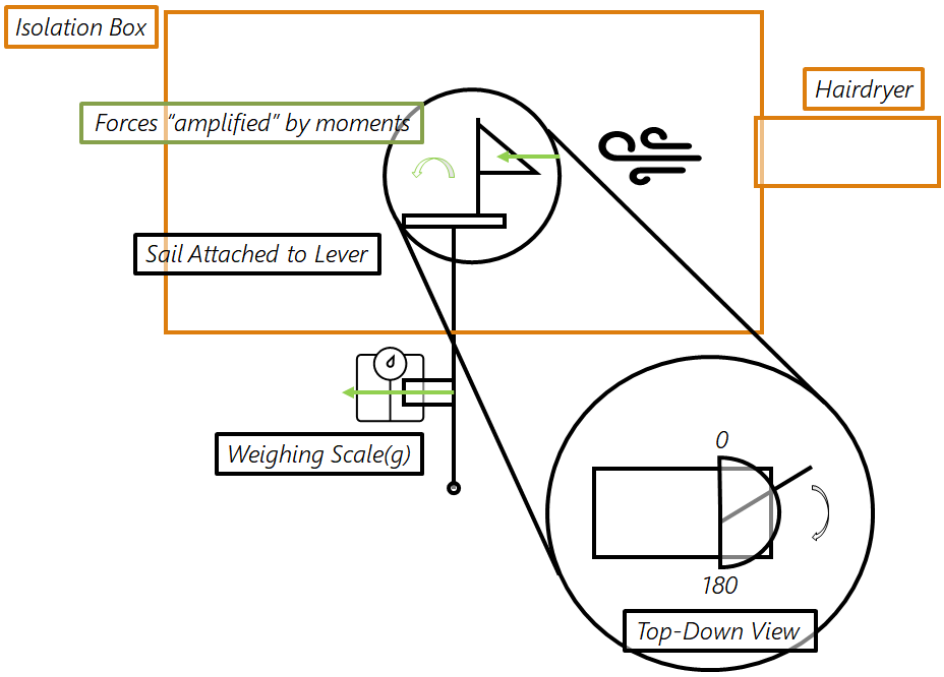

Figure 9.1: Schematic of the original wind tunnel

An isolation box is used to negate the effects of surrounding air currents such as wind from another fan, or the breathing of the tester. Strong wind is provided by a hairdryer at a constant angle and distance from the sail, aided in measurement by the placement of the box. As the wind

applies forces of lift and drag onto the sail, these forces are amplified through a lever, employing the concept of moments. The lever also serves to restrict the measured force in 1 direction at a time, so that the force can be measured as a vector, with both magnitude and direction. This transmitted force is then measured by a weighing scale, where it can be converted into a force measurement through mathematical manipulation. The position of the weighing scale and the direction of the lever can be adjusted, so as to measure the force both perpendicular and parallel to the wind.

Prototype I

With this schematic in mind, we began construction of the wind tunnel.

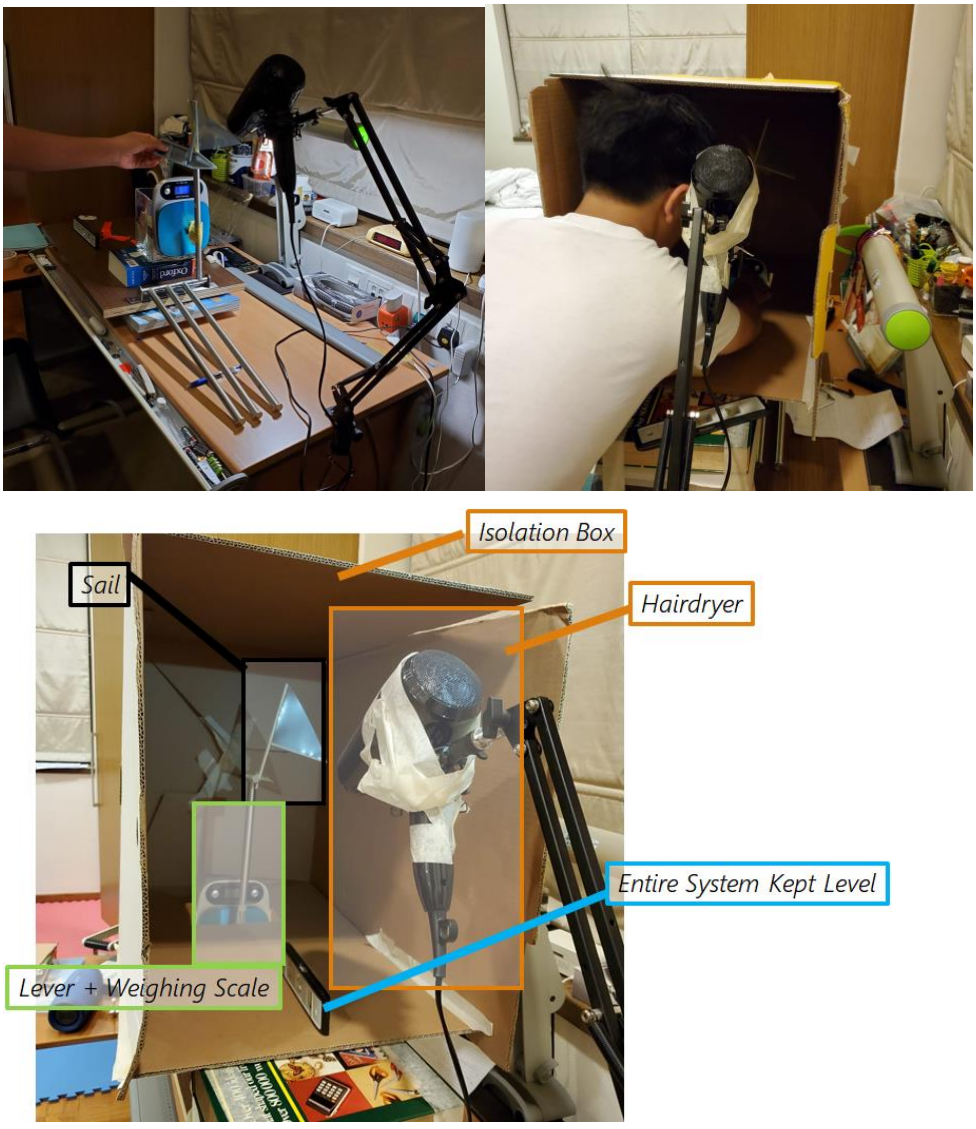

Figure 9.2: Images of the wind tunnel (pre-calibration)

The isolation box was made using a cardboard box, and a hairdryer was acquired. The stand for the hairdryer was repurposed from an old microphone stand one of our group members had. The lever was repurposed from a rotatable towel rack removed from a wall, with the tightness adjusted such that movement could be made as easily as possible. It was also sprayed with D-40 Lubricant so as to reduce the effect of friction. The weighing scale used was a kitchen scale, capable of measuring masses to a precision of 1g.

Great care was taken to calibrate, record, and standardise the dimensions of the wind tunnel. Measurements of the original setup of the wind tunnel were made using this improvised device, which allows lengths to be measured while making each part of the setup level, and measuring lengths straight. (e.g. the length between the nozzle of the hairdryer and the sail)

This “measurement” schematic is shown here, and all other recreations of the wind tunnel was built and calibrated based on these specifications:

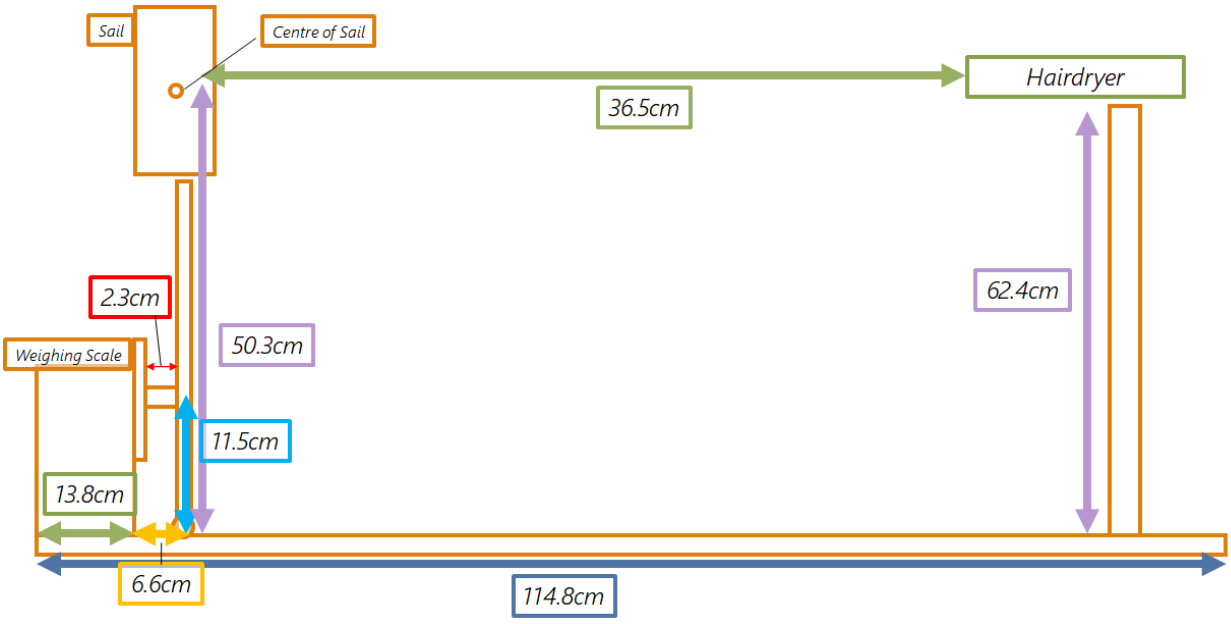

Figure 9.3: Specifications of the Wind Tunnel

Using these specifications, we can obtain the conversion of 1 gram ≈ 0.002243 Newtons. As the scale’s precision is 1 gram, this means that our device can theoretically measure forces of precision up to 2 mN.

Improvements

With the responsibility of having such a high precision bestowed upon us, it is now our job to make these measurements as accurate as possible, so as not to let the precision we have achieved go to waste. When performing a preliminary test of the sail at different wind angles, we observed a surprising trend.

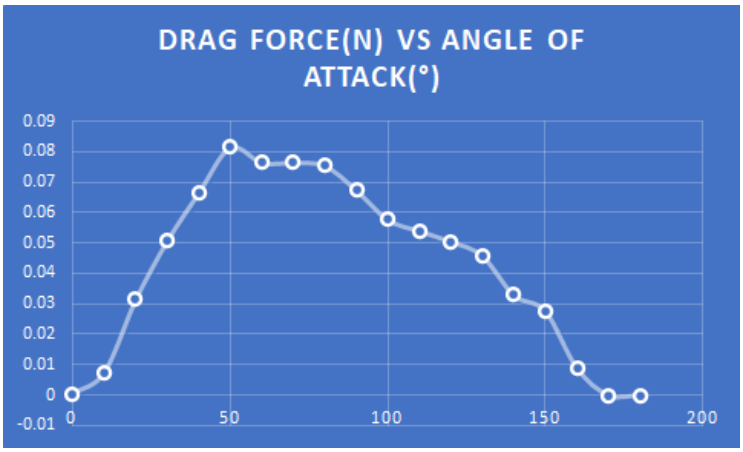

Figure 9.4: Initial graph of drag force against angle of attack experienced by sail

As you can see, the graph for drag force hit its peak at a 50° angle, contrary to the expected angle of about 90 degrees. Through a qualitative viewing of the test, we observed the following issues about the device that connects the sail to the lever, which may have led to this discrepancy:

1. At higher drag forces, the sail is pushed back in such a way that it “leans backward”, like so:

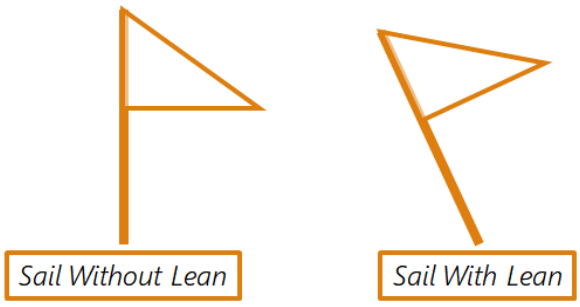

   This obviously affects the way in which the air interacts with the sail, and changes the reference area of the sail, thus decreasing both lift and drag measured
2. With higher drag forces, the sail begins to turn, changing the AoA (the independent variable) while the force is being measured.
3. Accurate turning of the sail to a given AoA is difficult — the original method of drawing a line down the sail and lining it to a small drawn protractor scale was shaky and inaccurate, due to the large room for human error in numerous precise steps. It also took a significant

amount of time to adjust the sail's AoA, which would have made the many measurements necessary hellish to accomplish.

Through brainstorming, we came up with the following solutions to the problems:
For problems 1 and 2, both these problems stem from issues with the structural stability of the device connecting the sail to the lever. This is to be expected as it was made of corrugated cardboard, which bends easily. Additionally, we only used 1 layer of cardboard in the beginning, hence the problems with leaning and turning. In order to fix the leaning problem, we layered the cardboard with 2 layers:

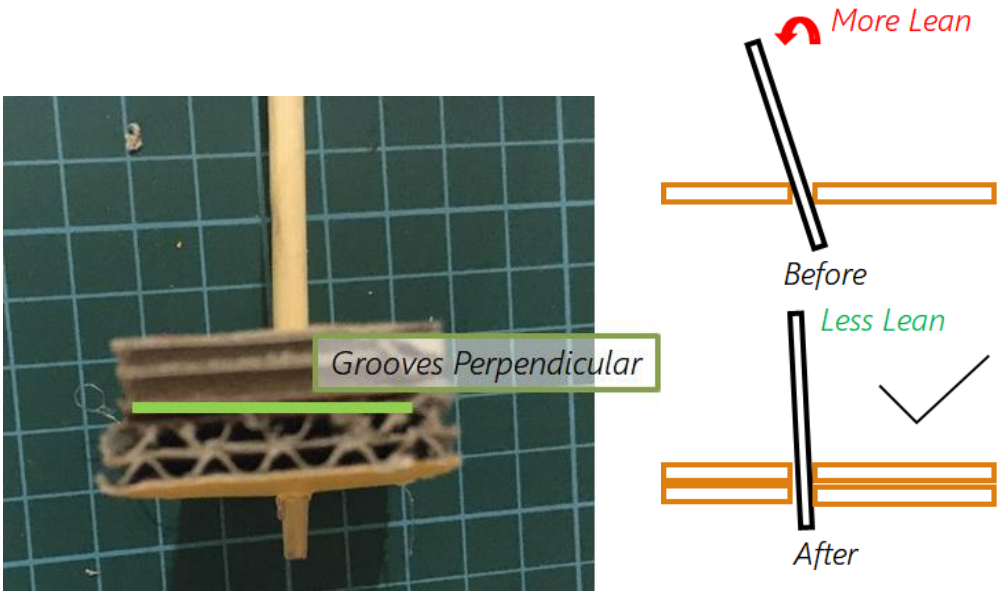

Figure 9.5: Solution to problems 1 and 2

This mitigates the issue of leaning, as there is now a greater surface in resistance to this motion. Additionally, the corrugated cardboard slices are lined perpendicularly to each other; this is as corrugated cardboard tends to be weaker and allow more motion in 1 direction, perpendicular to its "grooves". By pasting the sheets perpendicular to each other, we can use the concept of mutual scaffolding, vastly increasing the structural stability of the cardboard in both directions. Finally, the cardboard was cut using a penknife, instead of scissors. The combination of the sharper edge and one-way motion allowed for more cutting and less compression of the corrugated cardboard, which allows the cardboard to be stronger.

For the problem of turning, the sail was attached to a wooden chopstick, which gets narrower at the edge. When the chopstick pierces the cardboard, it produces a wedge, and thus can be

pushed in to be made tighter and conversely pulled out to be loosened enough for tuning. After adjusting the sail angle, we just have to push the sail a bit into the cardboard, and it is held tightly there.

In order to streamline the sail adjustment process, a novel method was devised. Firstly, the scale of a protractor was copied onto a piece of paper, and the paper was pasted onto the cardboard sheet, before being pierced in the centre by the chopstick. Next, a pocket torchlight was shone above the sail. Whenever we wish to adjust the sail angle, we can commence the following process:

1. Align the shadow of the mast of the sail (the centre of the protractor circle) with the actual mast of the sail. The light should now be directly above the mast.
2. Move the sail up to loosen it, then move it to the desired angle by aligning the centre shadow of the sail with that angle.
3. Push the sail back into the cardboard.

This method uses the concept that light travels in straight lines to deal with parallax error. The error here is about the size of the shadow — it is up to human judgement to decide where the centre of the shadow is. However, the shadow can be made sufficiently small such that the error in angle is much less than 1°.

As such, our wind tunnel is now complete, with a streamlined and efficient method for data collection.

<u>Final Material List</u>

Cardboard Box (significantly wider than the size of the sail)
Corrugated Cardboard Strips
Chopsticks
Hair Dryer
Weighing Scale (1g precision)
Weighing Scale Horizontal Mount
Rotatable Towel Rack
Wooden Plank
Rigid Block
Duct Tape

Sail Adjustment Mechanism

As the mast was provided with the boat that was given to us, we had to find a way to attach the sail to the boat at variable angles of attack, and in a secure manner. For this, a sail adjustment mechanism was proposed, refined, designed, and 3D-printed.

Here is an image of the device's STL file, as well as the device itself:

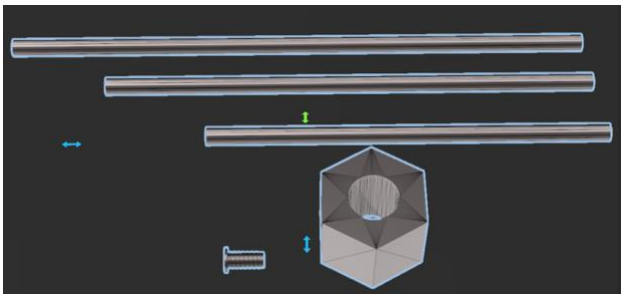

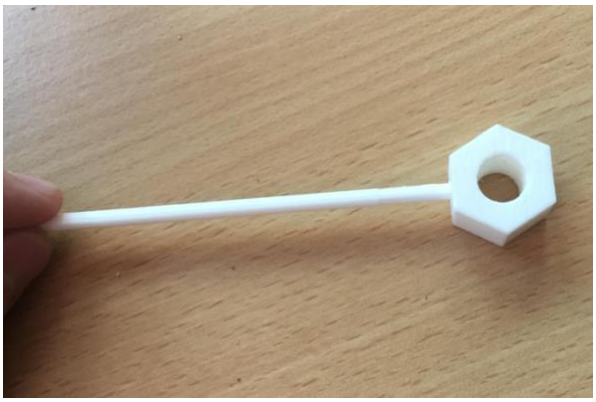

Figure 9.7: 3D-printed sail adjustment mechanism

The concept is as as follows:

The hexagonal device goes through the mast of the sail. (it is 3D-printed to fit perfectly, with a bit of leeway) It can be turned easily due to its hexagonal shape. 3 sail-holders are printed to fit into a hole in the hexagonal device, with a slit in each of them that allows the sail to be slotted in and taken back out easily. Finally, there is another hole in the hexagonal device for the placement of a screw there, allowing the device to be secured and loosened with ease, so that it does not slip when the sail is being blown, and it can easily turn when we want to adjust the angle. When we wish to change the sail length, we simply have to remove the current sail-holder and substitute it with another one of the appropriate length, then slot the sail into the holder. When we wish to adjust the sail angle, all we have to do is loosen the screw, turn the hexagonal device, and then retighten the screw, to keep the device in place.

Some improvements that we would make, given more time and resources, would be to use a stronger 3d printing material, such as a polycarbonate filament. This is as our sail-holders were quite bendy and structurally weak — we had to use a lower wind speed in our Testing and Evaluation section (Section 5) for fear that it might break. Additionally, we would have made the hexagonal device smaller, and lighter, as it turned out larger and heavier than expected, impeding the motion of the boat. However, we still believe this device was valuable and successful in that it allowed us to easily adjust sail angles and lengths on the boat, which worked well in practice.

Towing Tank

In order to find the drag of the hull and the keel, a towing tank was created. This tank operates on a principle of dragging the boat through the water, following which a force could be measured.

Initial Prototype

Our initial plan was extremely straightforward: we simply placed a boat in a water, and dragged it with a Newton Meter at a constant speed. From this, we can look at the reading of the Newton Meter and get an accurate reading of the drag forces acting on the boat and the keel. However, this became problematic for 2 reasons:

1. There was no accurate way to ensure that we were pulling the boat at a constant speed, and hence no way to ensure the accuracy of the drag force on the boat.
2. The Newton Meter was not sensitive enough to measure the extremely small drag forces. The Newton Meter we had was an electronic one, capable of measuring to 0.1N. However, this would turn out to be insufficient, especially when attempting to measure the differences in drag forces of different keel designs.

Hence, this initial method to optimise the keel-water interface was not successful.

Constructing the Towing Tank

The first version of the towing tank is close to the current model of the towing tank, barring a few changes which we will outline later. The principle of the towing tank is relatively straightforward: using a constant force, pull the boat and then note the time taken for it to travel a fixed distance. We initially used a normal phone, which could film at 30 frames per second.

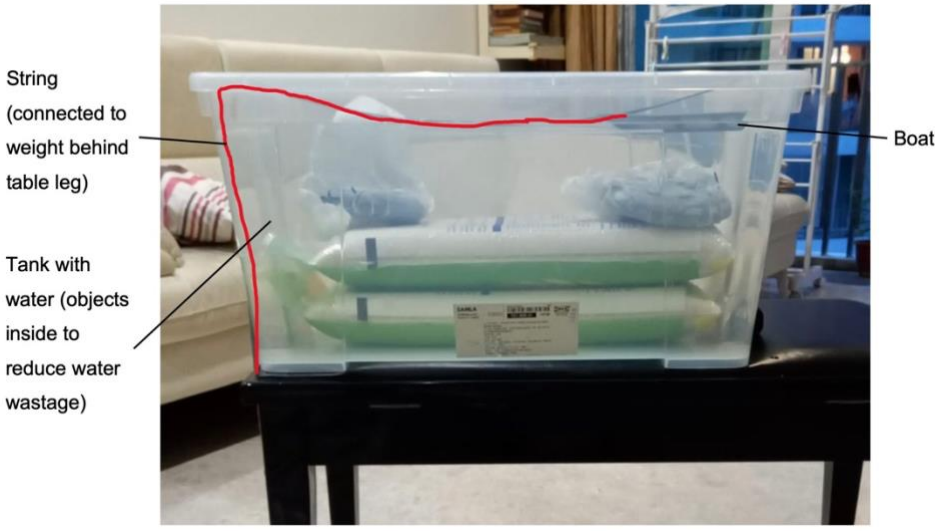

Figure 9.8: Labelled Diagram of Towing Tank v1

However, after analysing the footage, we realised that we could further improve on the set-up in the following ways:

1. Because there is an angle at which the string pulls the boat, this “lifts” the boat out of the water, leading to inaccurate results. Hence, a hole should be made slightly above the water level, with the string going through the hole, to minimise this effect from occurring.
2. When we made a hole in the box, the string would keep getting stuck there as it would get caught on the bottom edge of the hole. Hence, to keep the string straight as it moves through the hole (reducing friction), we used a fulcrum (a roll of tape), which allowed the string to move freely and our setup to work.
3. The camera recording at 30 frames per second, while reasonably accurate, could not allow us to make precise measurements of time taken to move the distance of 50cm, given that such times were less than 1.00s. Hence, we decided to use a slow-motion camera (iPhone slow-motion feature), which records at 240 frames per second.

Hence, this is a diagram of the final set-up:

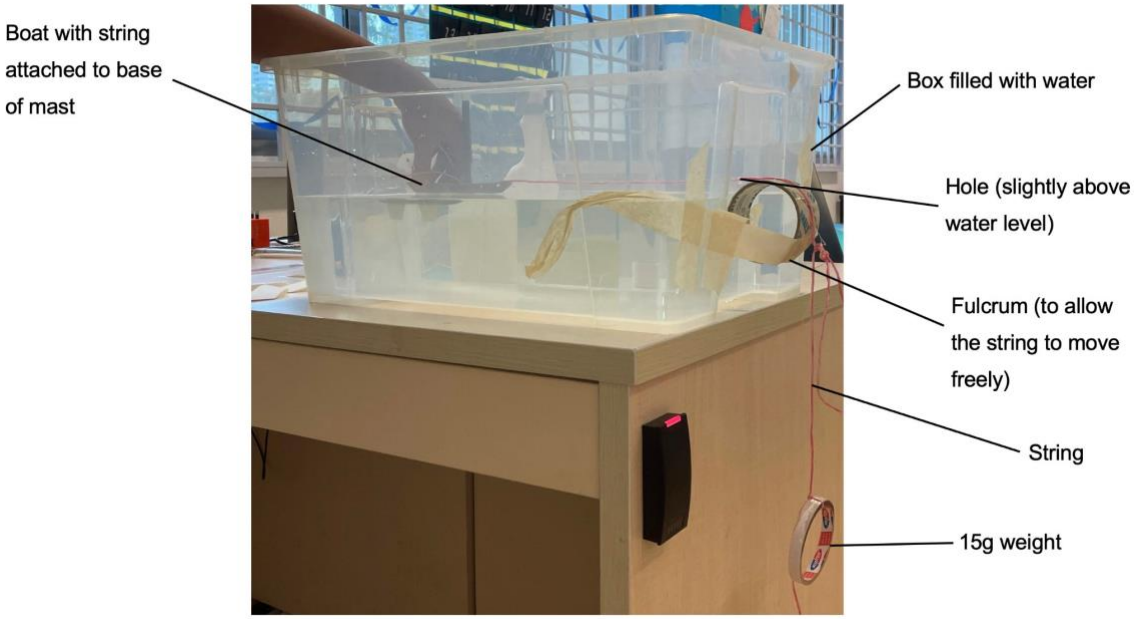

Figure 9.9: Side view of the final experimental set-up

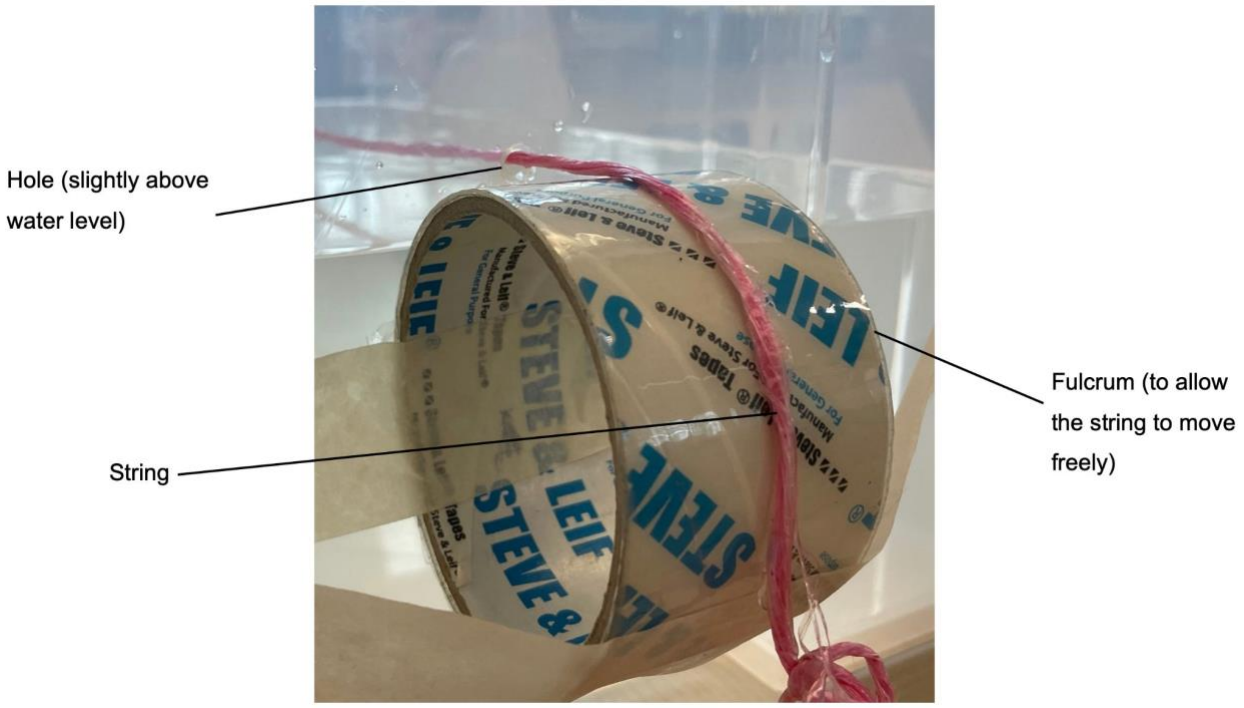

Figure 9.10: A close-up of the hole in the box and its friction-reducing mechanism

While this set-up was sufficiently able to measure the effects of drag force through counting the number of frames to an accuracy of 0.00417s, before using simple kinematics and dynamics to estimate the drag force on the object. However, there are still certain limitations to the set up. For one, we were simply using our hands to release the object, which could affect experimental results if we released it unevenly. In future, we could design a release mechanism for the boat, such that the results collected are more accurate. As the exact frame when the boat is released is difficult to ascertain, having a light bulb that lights up with the release of the boat in the mechanism would be helpful as well. Additionally, the waves created by the boats motion could certainly have reflected back to interact with the boat, knocking it off course — we noticed that while the motion was kept fast, some waves still reflected off the edge of the tank back to the boat. As such, having a larger box, and a longer testing distance would attenuate the issue of reflection of the wave, and reduce the effect of random error by making the results more pronounced.

10 APPENDIX C: EXPERIMENTAL DESIGNS + RESULTS + DISCUSSION

10.1 Keith Chan (Angle of Attack)

Aim of Experiment

The aim of the experiment is not to find 1 optimal Angle of Attack (AoA), but rather the optimal AoAs for any given wind direction. AoA is defined relative to the wind direction, as shown in the following image:

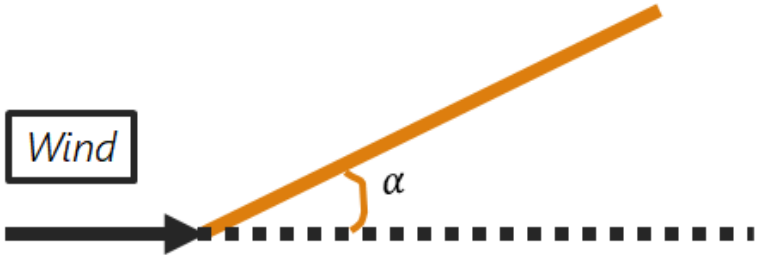

The end goal is to maximise the driving force of the boat given a certain wind angle by examining the lift and drag forces at different AoAs, so as to maximise the velocity of the boat, and hence minimise the time taken for the boat to travel 30cm.

Key Variables:

Angle of Attack of Sail to Wind (Independent Variable, changed)

Lift Force, Force perpendicular to wind direction (Dependent Variable, measured)

Drag Force, Force parallel to wind direction (Dependent Variable, measured)

Surrounding Airflow, Wind Speed, Tilt/Leaning/Twisting of Sail (Independent Variables, kept constant)

Sail Area, as mentioned in other experiment (Independent Variable, kept constant)

Wind Direction is also kept constant here, as we believe we can use equations to extrapolate our data out to any given wind direction.

Apparatus and materials Needed:

Wind Tunnel with a weighing scale and enclosed environment (See Appendix B part 1 for construction + Material List here)

1 Clear Plastic Folder

1 pair of Wooden Chopsticks

Pocket Torchlight

Penknife

Glue Gun

String

Experimental Procedure:

(In this procedure, the more pointed tip of the chopstick will be referred to as **Tip Pointy** and the blunter tip of the chopstick will be referred to as **Tip Blunt**)

Fig. 10.1.1: Labelling the different ends of a chopstick

Sail construction

1. Using the penknife, cut a triangular sail with dimensions 10cm by 10cm, as seen in Fig. 10.1.2

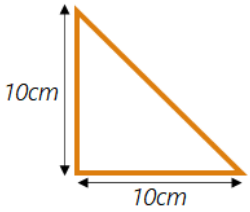

Fig. 10.1.2: Sail Specs

2. Using the penknife, cut 1 of the 2 wooden chopsticks at the point 10cm away from **Tip Pointy**. Keep the side with **Tip Pointy**, and discard the one with **Tip Blunt**. (Fig. 10.1.3)

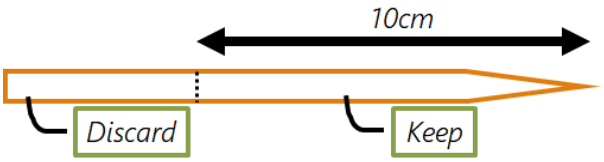

Fig. 10.1.3: First Cut

3. With the glue gun, glue the cut chopstick to the uncut chopstick 10cm from **Tip Blunt** of the uncut chopstick, with **Tip Pointy** of the cut chopstick facing outwards. Wait for the glue to dry. (Fig. 10.1.4)

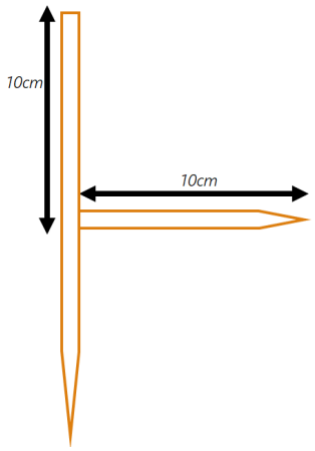

Fig. 10.1.4: Sail Frame

4. With the glue gun, glue the edges of the sail to the chopstick frame constructed in steps 2 & 3, and wait for it to dry.

Drag Measurement

5. Put the wind tunnel into drag measurement form. (See: Appendix B)
6. Place the sail into the sail holding device of the wind tunnel, and align it to the 0° marking of the sail holding device with the help of the pocket torch (See: Appendix B)
7. Hold one end of the string at the centre of the nozzle of the hairdryer(of the wind tunnel), and the other at the mast of the sail, to ensure that the airflow from the hairdryer lines up with the mast of the sail. Adjust the hairdryer or the sail holding device if necessary, such that the airflow lines up.
8. Turn on the hairdryer, and use the weighing scale of the wind tunnel to record a reading of the mass measured on the weighing scale (in grams).
9. With the help of the pocket torch , align the sail to the 10 degree marking and repeat step 8. Repeat this step for the 20°, 30°, 40°, 50°, 60°, 70°, 80°, 90°, 100°, 110°, 120°, 130°, 140°, 150°, 160°, 170° and 180°, for a total of 18 different angles of attack**.**
10. Repeat Step 9 three times, and calculate the average and standard error of the readings.
11. Construct an excel spreadsheet of the results obtained. For each value measured x, scale it into a force through the formula $\frac{11.5}{50.5} \times \frac{9.81x}{1000}$ [From the conversion equation in the wind tunnel Schematic]
12. Plot the acquired results in Step 11.

Lift Measurement

13. Put the wind tunnel into lift measurement form. (See: Appendix B)

14. Repeat steps 6 - 8
15. Repeat step 9, but only repeat step 8 for 20°, 30°, 40°, 50°, 60°, 70°, 80°, 90°, for a total of 9 different angles of attack.
16. Repeat Step 15 three times, and calculate the average and standard error of the readings.
17. Construct an excel spreadsheet of the results obtained. For each value measured x, scale it into a force through the formula $\frac{11.5}{50.5} \times \frac{9.81x}{1000}$ [From the conversion equation in the wind tunnel Schematic]
18. Plot the acquired results in Step 17.

Results + Discussion

Angle (degrees)	Reading 1 (g)	Reading 2 (g)	Reading 3 (g)	Drag 1 (N)	Drag 2 (N)	Drag 3 (N)	Average Drag (N)	STDEV
0	0	0	2	0	0	0.004486	0.001495	0.001495229
10	6	5	8	0.013457	0.011214	0.017943	0.014205	0.001978002
20	19	20	17	0.042614	0.044857	0.038128	0.041866	0.001978002
30	34	36	35	0.076257	0.080742	0.0785	0.0785	0.001294906
40	40	44	43	0.089714	0.098685	0.096442	0.094947	0.002695562
50	46	54	50	0.103171	0.121114	0.112142	0.112142	0.005179624
60	47	56	58	0.105414	0.125599	0.130085	0.120366	0.007587457
70	45	53	54	0.100928	0.118871	0.121114	0.113637	0.006387619
80	47	53	51	0.105414	0.118871	0.114385	0.11289	0.003956003
90	53	64	44	0.118871	0.143542	0.098685	0.120366	0.012970624
100	46	37	40	0.103171	0.082985	0.089714	0.091957	0.005934005
110	32	34	33	0.071771	0.076257	0.074014	0.074014	0.001294906
120	30	31	31	0.067285	0.069528	0.069528	0.068781	0.000747614
130	24	26	27	0.053828	0.058314	0.060557	0.057566	0.001978002
140	20	22	24	0.044857	0.049343	0.053828	0.049343	0.002589812
150	8	10	11	0.017943	0.022428	0.024671	0.021681	0.001978002

160	0	6	4	0	0.013457	0.008971	0.007476	0.003956003
170	1	2	4	0.002243	0.004486	0.008971	0.005233	0.001978002
180	0	0	0	0	0	0	0	0

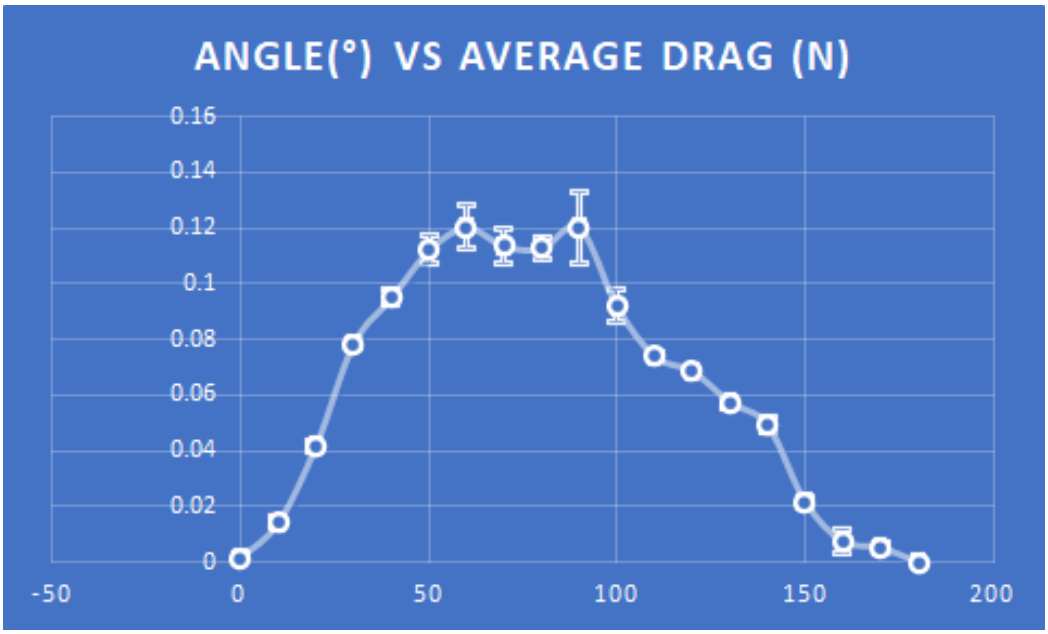

Figure 10.1.5: Drag - AoA Table + Graph, range 0 - 180, with error bars (10 cm)

As can be seen from the graph, the average drag is around 0N at 0°, and increases with AoA until around 90°, before decreasing again, hitting 0N at 180°. This agrees with our background reading on the subject, as the flow becomes most deflected at around 90° AoA. A reason why the drag decreased at 90°, however, might be due to the issue of leaning as mentioned in Appendix B. Whilst we tried to mitigate this issue by strengthening the cardboard, the issue may still have persisted.

Angle (degrees)	**Reading 1 (g)**	**Reading 2 (g)**	**Reading 3 (g)**	**Lift 1**	**Lift 2**	**Lift 3**	**Average Lift**	**STDEV**
0	0	2	1	0	0.004486	0.002243	0.002243	0.001295
10	3	4	6	0.006729	0.008971	0.013457	0.009719	0.001978
20	8	9	12	0.017943	0.020186	0.026914	0.021681	0.002696
30	25	26	30	0.056071	0.058314	0.067285	0.060557	0.003426
40	29	27	30	0.065042	0.060557	0.067285	0.064295	0.001978
50	28	24	27	0.0628	0.053828	0.060557	0.059062	0.002696

60	27	25	26	0.060557	0.056071	0.058314	0.058314	0.001295
70	19	19	20	0.042614	0.042614	0.044857	0.043362	0.000748
80	7	6	6	0.0157	0.013457	0.013457	0.014205	0.000748
90	0	0	0	0	0	0	0	0

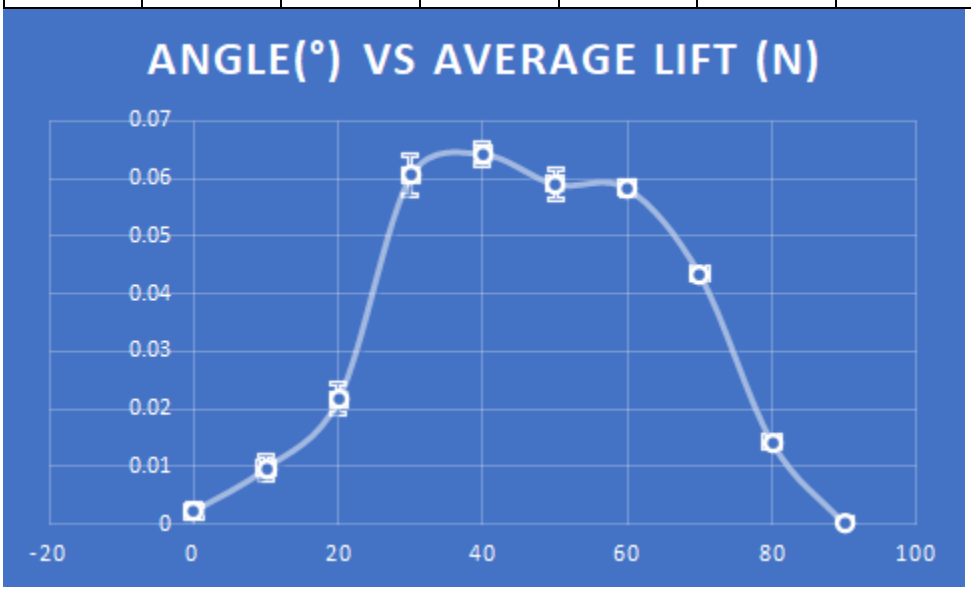

Figure 10.1.6: Lift - AoA Table + Graph, range 0 - 90, with error bars (10 cm)

As can be seen from the graph, the average lift is about 0N at 0° AoA, and rapidly increases to 0.065N at around 35° AoA, before decreasing again. This agrees with our background reading, as we expect the lift to increase with AoA due to the increase in flow curvature, before decreasing again due to the effects of turbulence and stalling. However, what is surprising is how gradual the decrease in lift after it hits its stall point is. This could be as there is still significant curvature and lift produced by the upper surface of the sail during the stall.

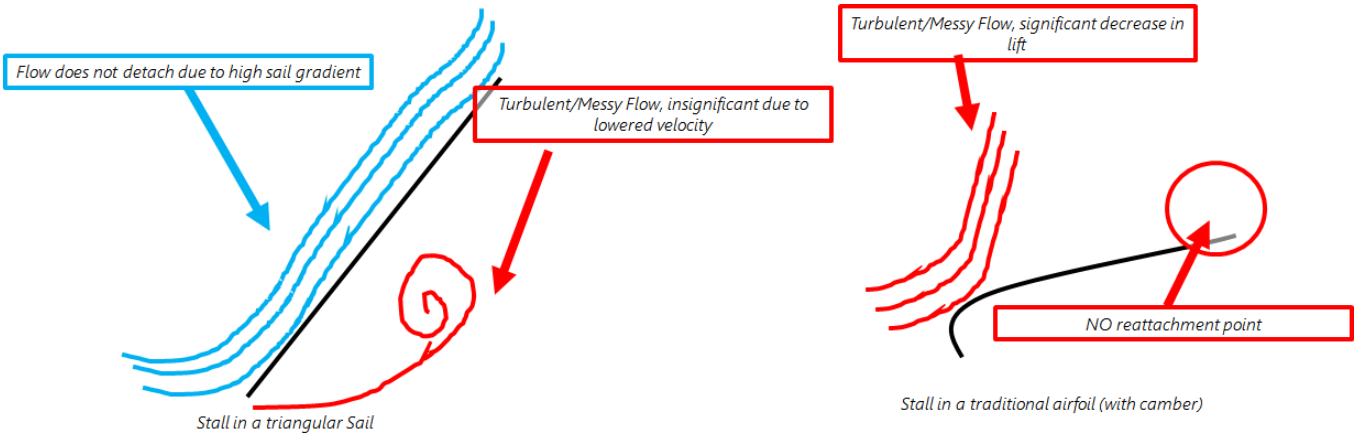

Fig. 10.1.7: Stall in our triangular Sail with a "hard" leading edge, vs that of a normal airfoil

Another thing that is surprising is how much lower our lift values are than our drag values - in a normal sail/airfoil, we would expect lift to have a peak about 3 times that of drag. Once again, this is likely due to the thinness and the lack of camber of our sail, which both are factors that should drastically increase the lift.

To validate the graphs for the 10cm sail, I also conducted a similar test with the 5cm sail, and plotted their results similarly:

Angle (degrees)	Reading 1 (g)	Reading 2 (g)	Reading 3 (g)	Drag 1	Drag 2	Drag 3	Average Drag	STDEV
0	0	0	0	0	0	0	0	0
10	3	4	3	0.006729	0.008971	0.006729	0.007476	0.000747614
20	13	15	14	0.029157	0.033643	0.0314	0.0314	0.001294906
30	23	25	22	0.051585	0.056071	0.049343	0.052333	0.001978002
40	30	30	29	0.067285	0.067285	0.065042	0.066538	0.000747614
50	35	38	36	0.0785	0.085228	0.080742	0.08149	0.001978002
60	40	43	37	0.089714	0.096442	0.082985	0.089714	0.003884718
70	42	43	42	0.094199	0.096442	0.094199	0.094947	0.000747614
80	36	38	36	0.080742	0.085228	0.080742	0.082238	0.001495229
90	39	40	37	0.087471	0.089714	0.082985	0.086723	0.001978002
100	34	35	35	0.076257	0.0785	0.0785	0.077752	0.000747614
110	34	35	34	0.076257	0.0785	0.076257	0.077004	0.000747614
120	26	29	30	0.058314	0.065042	0.067285	0.063547	0.002695562
130	22	24	23	0.049343	0.053828	0.051585	0.051585	0.001294906
140	13	16	15	0.029157	0.035885	0.033643	0.032895	0.001978002
150	12	13	12	0.026914	0.029157	0.026914	0.027662	0.000747614
160	3	5	4	0.006729	0.011214	0.008971	0.008971	0.001294906
170	0	0	0	0	0	0	0	0
180	0	0	0	0	0	0	0	0

Figure 10.1.8: Drag - AoA Table, range 0 - 180, with error bars (5 cm)

Angle(degrees)	Reading 1 (g)	Reading 2 (g)	Reading 3 (g)	Lift 1	Lift 2	Lift 3	Average Lift	STDEV
0	0	0	1	0	0	0.002243	0.000748	0.000748
10	8	7	9	0.017943	0.0157	0.020186	0.017943	0.001295
20	15	16	18	0.033643	0.035885	0.040371	0.036633	0.001978
30	19	24	26	0.042614	0.053828	0.058314	0.051585	0.004669
40	26	27	23	0.058314	0.060557	0.051585	0.056819	0.002696
50	23	23	22	0.051585	0.051585	0.049343	0.050838	0.000748
60	14	17	15	0.0314	0.038128	0.033643	0.03439	0.001978
70	10	9	8	0.022428	0.020186	0.017943	0.020186	0.001295
80	6	7	6	0.013457	0.0157	0.013457	0.014205	0.000748
90	4	3	3	0.008971	0.006729	0.006729	0.007476	0.000748

Figure 10.1.9: Lift - AoA Table, range 0 - 180, with error bars (5 cm)

Comparison of the 4 obtained graphs:

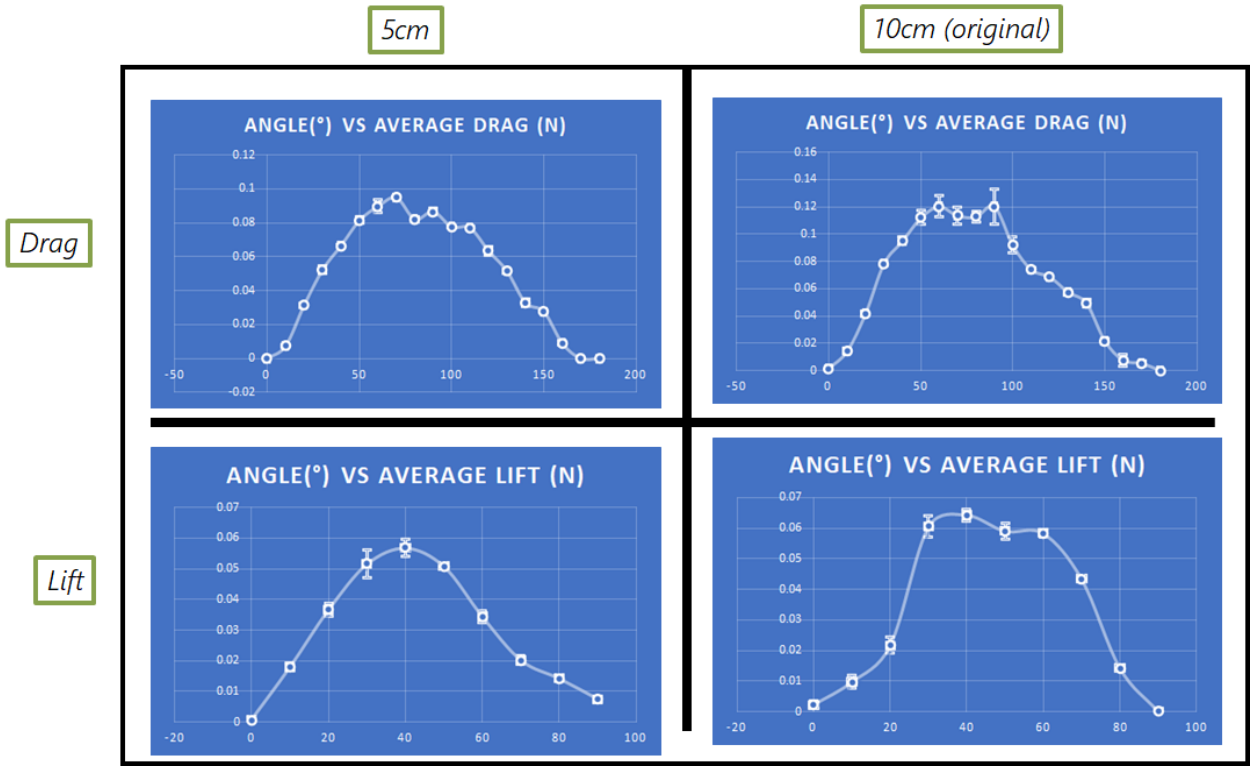

Figure 10.1.10: Comparison of 4 graphs obtained above

We see extremely similar trends here, save the smaller force readings. What is interesting here is that there is only 1 peak for lift in the 5cm graph - this suggests that the dip in the rest of the graphs was indeed due to the error caused by “leaning”. Since the forces for lift in the 5cm sail are so low, the sail likely did not lean as much, and thus the difference was less noticeable.

Possible Sources of Error Include:

- The aforementioned “leaning” effect - Whilst much effort was taken to mitigate this problem, it still persists for very high forces, and the dips in the data where we expect peak forces to be could be a result of this, as evidenced by the cross comparison with the 5cm sail, which had a weaker force and thus no dip. For future improvement, I could try using a weaker wind source that would cause less leaning, or use more layers of cardboard to prevent leaning from happening.
- The sail may not have been calibrated accurately - this was heavily mitigated by the streamlined and novel sail calibration method that we used, which had a low margin of error of under 1°
- There may have been interference from outside wind sources - this was also heavily mitigated by the protective isolating box.
- The different parts of the setup may have moved about during the experiment, which would have changed the wind speed at the sail, and the wind direction, which should be in the same direction as the 0° marking on the sail adjustment mechanism. However, I believe this was also well mitigated with the precise and conscientious marking out of lengths in the schematic - these lengths were checked before and after the experiment, without much noticeable deviation.

All in all, apart from the systematic error of leaning, which we tried to avoid but still showed up in our final results, I believe that most of the random of the sources of error were dealt with, as evidenced by the low standard errors that we calculated (See: Fig. [] for error bars)

There is 1 point in the 10cm, drag graph which has a high error bar, which may be due to an anomalous reading.

Conclusion:

With this data on the lift and drag values at each AoA, we can plot the equation for driving force, given a constant wind direction:

$$T = Lsin\,\beta - Dcos\,\beta = L(sin\,\beta - \frac{D}{L}cos\,\beta)$$

Now, we have an excel page, with an input for a wind direction, that then provides the graph of AoA to driving force for the given wind direction.

	Angle(degr	Lift	Drag	Driving force		Wind Dir
	0	0.002243	0.001495	0.002243		1.570796
	10	0.009719	0.014205	0.009719		
	20	0.021681	0.041866	0.021681		
	30	0.060557	0.0785	0.060557		
	40	0.064295	0.094947	0.064295		
	50	0.059062	0.112142	0.059062		
	60	0.058314	0.120366	0.058314		
	70	0.043362	0.113637	0.043362		
0	80	0.014205	0.11289	0.014205		
1	90	0	0.120366	-7.4E-18		
2	100	-0.0142	0.091957	-0.0142		
3	110	-0.04336	0.074014	-0.04336		
4	120	-0.05831	0.068781	-0.05831		
5	130	-0.05906	0.057566	-0.05906		
6	140	-0.06429	0.049343	-0.06429		
7	150	-0.06056	0.021681	-0.06056		
8	160	-0.02168	0.007476	-0.02168		
9	170	-0.00972	0.005233	-0.00972		
0	180	-0.00224	0	-0.002		
1						

Here, I have reflected the lift values about the 90° value and made them negative, which makes sense since the lift past 90° should just go in the opposite direction.

Let us run some examples with this code:

<u>At 45 degrees headwind (from the front):</u>

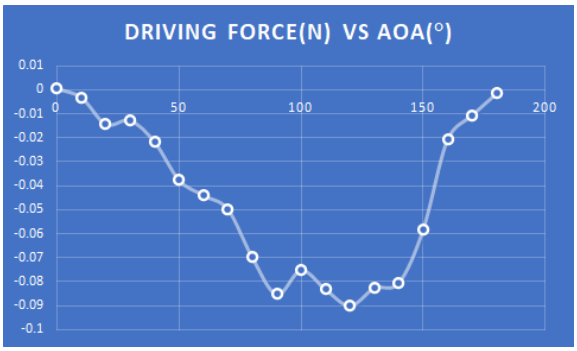

Figure 10.1.11: Graph of driving force against AoA at 45 degrees headwind

Majority of the graph is in the negatives, save a bit near 0° AoA. This makes sense, as it is difficult to sail towards the wind when it is travelling against you - the region where you are travelling forward, or the “pocket” as it is known to sailors, is very small. This type of sailing is known as “close haul”.

Below 45 degrees headwind (from the front)

At a 30° headwind, the driving force graph is entirely below the x-axis — It is impossible to move forward at this angle.

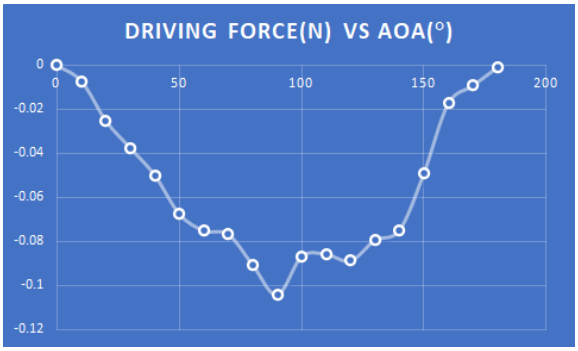

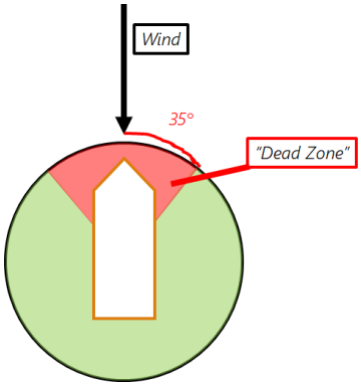

Figure 10.1.11: Graph of driving force against AoA at 30 degrees headwind

This is similar for all graphs below 35°. Therefore, the region 35° left and right of the wind is the “dead zone” - one cannot sail forward in that region.

90 degrees “Beam Reaching”

Sailing at 90 degrees to the wind direction is known as “Beam Reaching”. With our excel file, the graph of driving force is:

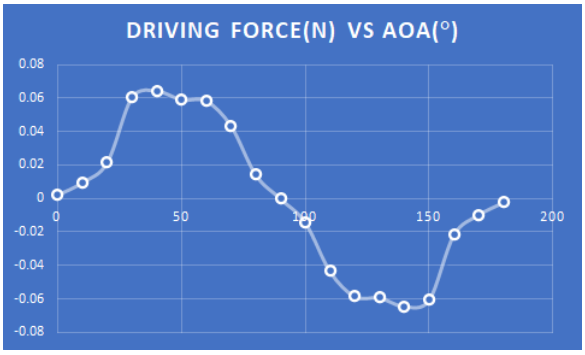

Figure 10.1.12: Graph of driving force against AoA at beam reaching

Notably, there are large positive and negative regions of the graph. This means that depending on the angle of our sail, we can travel in either direction relative to the wind, which makes sense physically.

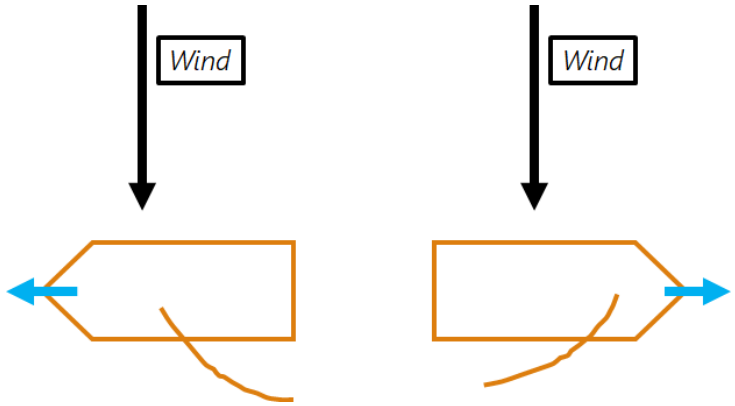

Fig. 10.1.13: The boat is able to sail equally well in both directions

Even though the driving force here is not the highest, this should be the configuration that gives the fastest theoretical speed over time — This is as the relative wind produced by the movement of the boat should not impede much with the driving force of the boat. We do not see such results in our experiment as our sail does not have curvature - thus Lift is much lower, and this movement of the boat is made less effective.

<u>180 Degrees Backwind</u>

With wind blowing from behind the boat, we observe the following graph:

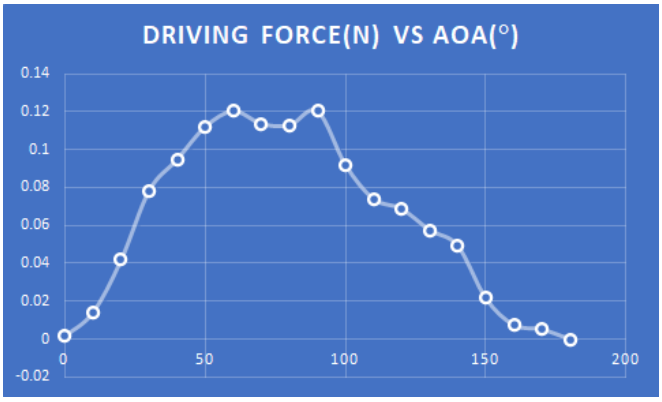

Figure 10.1.14: Graph of driving force against AoA at backwind

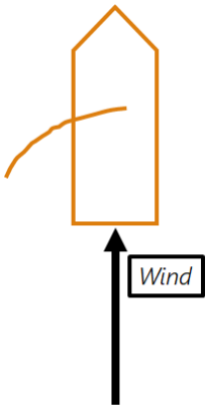

No matter what angle I put my sail at, the boat will have a driving force, which also makes intuitive sense.

Lift Drag Polar Diagram

The above results can be expressed by plotting the graph of Lift to Drag, with the AoA as "parametric" variable:

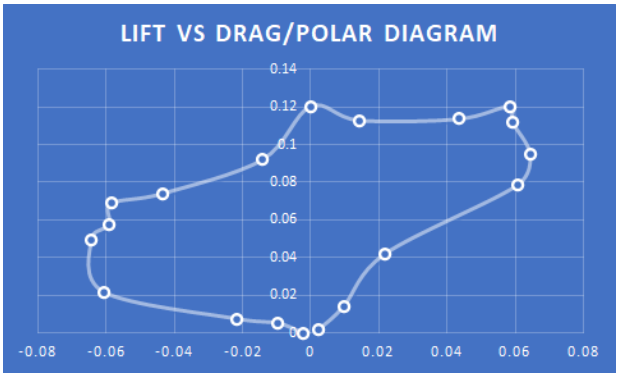

Figure 10.1.15: Lift to drag polar diagram

What is useful about this diagram is that it allows us to easily determine the sail setting that provides maximum driving force, given a wind angle. The method is as follows:

1. Let the wind direction originate from the negative side of the X-axis.
2. Indicate the boat with its intended travel direction relative to the wind direction. The angle between this direction and the X-axis should be β.
3. Draw a line in the positive XY direction, perpendicular to the intended direction of travel of the boat.
4. The line in the positive XY direction can be moved along the line of intended travel direction, until it is tangent to the Lift-Drag Polar curve.
5. The line between the point of contact and the origin provides us with the total aerodynamic force for maximum drag, and maximum drag and sail angle can be calculated from this.

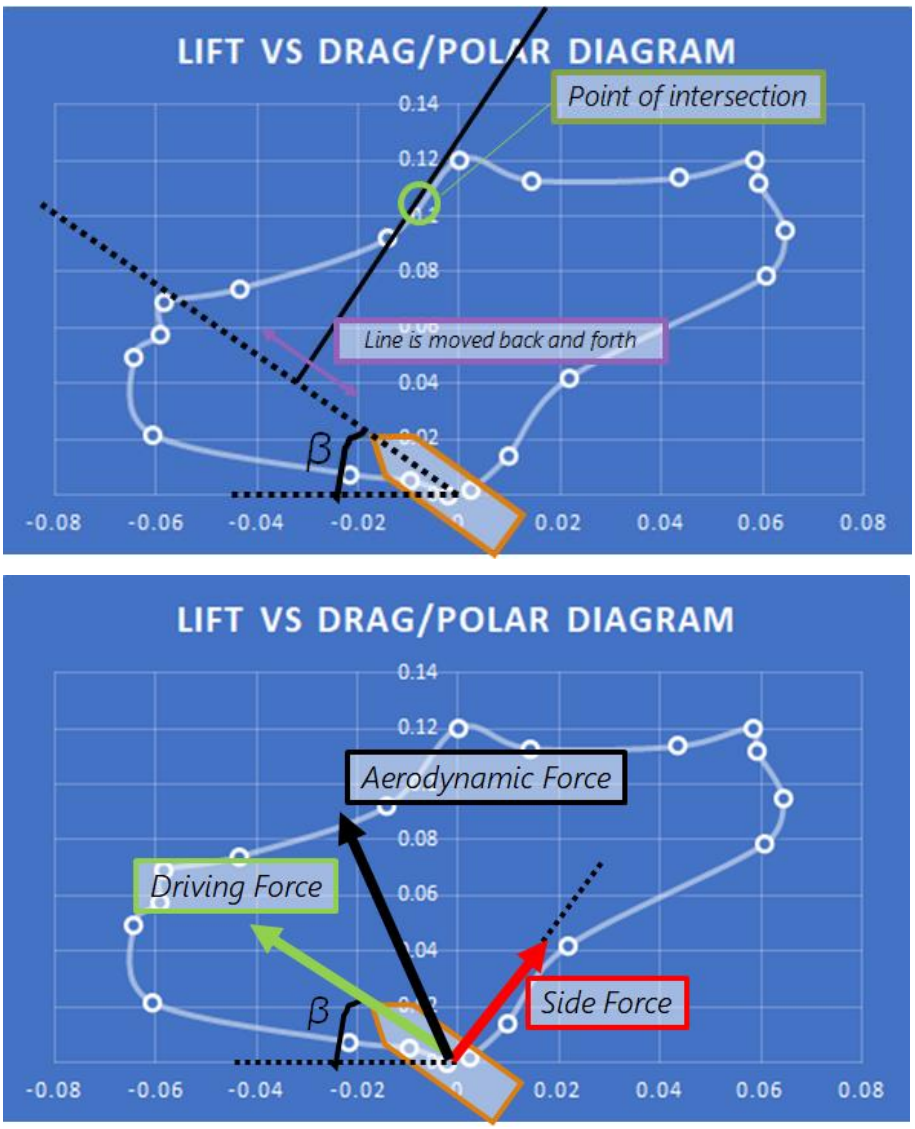

Figure 10.1.16: Using the Polar Diagram

This is a geometrical representation of solving the equation condition for the maximum driving force:

$$\frac{dD}{dL} = tan\,\beta$$

Side Force

For there to be a driving force, there will also be an aerodynamic side force, which must be counteracted. The formula for this side force is:

$$S = Lcos\,\beta + Dsin\,\beta$$

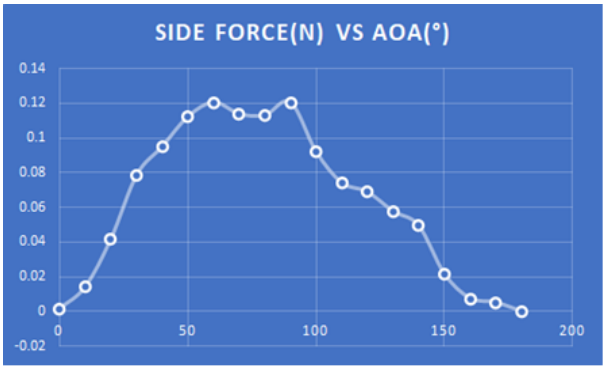

Side Force (90 degrees)

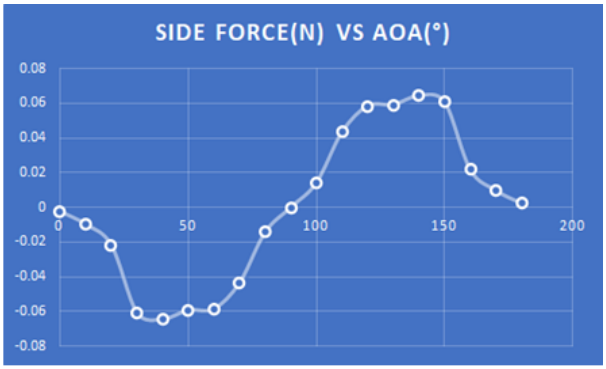

Side Force (180 degrees)

Figure 10.1.17: Graphs of side force at various wind angles

As we expect, there are lower side forces when blowing the ship from the back than when blowing at 90°. However, side forces are still significant from the back, when the sail is at an angle - it is only when the sail is parallel with the wind flow that there are no side forces, but also no driving force.

As we increase the total aerodynamic force, the driving force increases, but so does the side force, which is why it is important to have a good keel. This is seen in our evaluation and testing section (Section 5), where the 15cm sail, while providing good driving forces, caused the boat to capsize quickly, and thus was ultimately rendered ineffective.

In conclusion, I have experimentally characterised the Lift and Drag to AoA graphs for our sail, which scale linearly due to the Lift and Drag Equations - as the wing area, wind velocity and air density were all kept constant, we have effectively characterised the lift and drag coefficients (refer to Section 3). With these values, I have found and explained graphs of the driving force and side force, as well as made use of the technique of a *polar diagram* to show how the angle that gives the maximum driving force can be found.

All of the above data and computations can be found at this excel spreadsheet, downloadable on Github: *https://tinyurl.com/2021physpt-saildata*

Of note is the Lift+Drag page, which has an interactive input for wind direction in degrees. Please feel free to experiment with it and observe the changes in the graphs created.

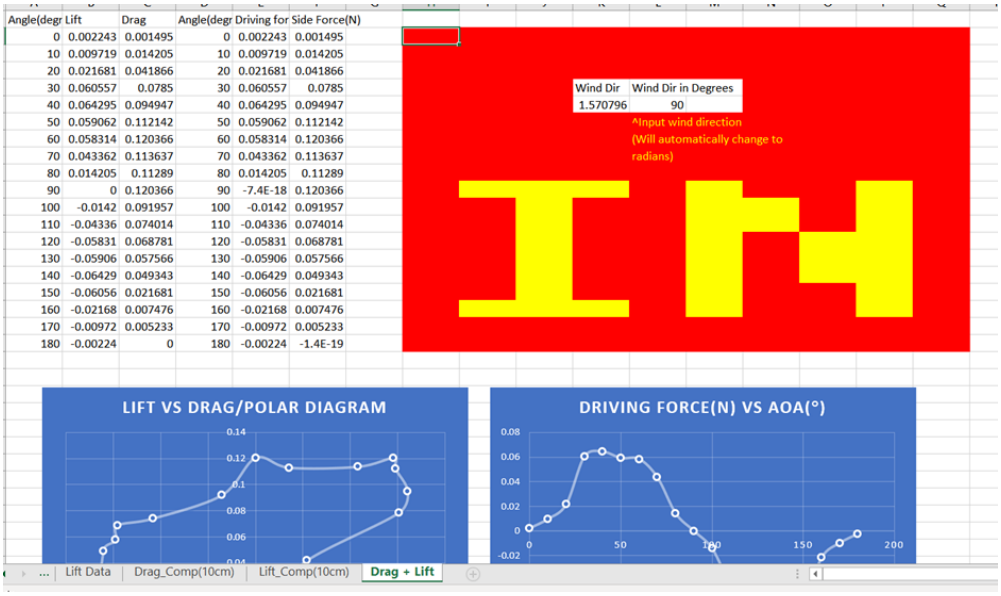

Therefore, I have sufficiently secured the aims of the experiment, which is to find the optimal AoA to maximise driving force, given any wind direction.

A major underlying assumption here is that a maximum driving force necessarily translates into faster movement — this can turn out to be inaccurate due to some issues mentioned in Appendix A, such as the relative wind of the boat in its movement. However, due to the short timescales for the boat to complete a 30cm lap observed in the Test and Evaluation section, I believe the effect of relative wind to be negligible in my test. Another thing that could be improved is that, while this test is able to account for the unspecified wind direction, it does not account for the unspecified wind speed/strength. I used a strong hairdryer as a wind source in my experiment, as it produced more pronounced differences in the forces measured such that they could be measured and graphed more precisely. However, the actual scenario presented could have a weaker wind source such as a fan, or a stronger wind source such as a leaf blower. This would certainly change the flow velocity of the wind at the sail, as well as the turbulence and Reynold's numbers of the flow, which would change my results. As such, accounting for wind speed could be a good idea in the future, although I am unable to provide any suggestions as to how this could be done.

10.2 Bennetton Ang (Length of sail)

Statement of Problem

To determine the optimal size of sail that maximises the drag and lift force exerted on the boat.

Key Variables

Length of sail

Constant Variables

Material of sail

Surrounding Airflow, Wind Speed, Tilt/Leaning/Twisting of Sail

Wind Direction

Apparatus and materials Needed:

Wind Tunnel (See Appendix B part 1)

Sail adjustment mechanism

3D Printed Boat

Plastic sheets cut into sails with lengths of 5cm, 10cm, and 15cm respectively

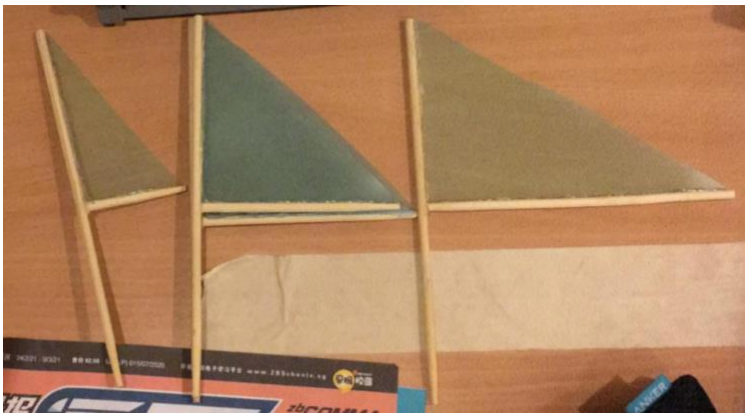

Figure 10.2.1: Image of the 3 sail lengths that we investigated (5cm, 10cm and 15cm)

Experimental Procedure:

1 The rigging device is attached to the boat

2 Sails are attached to the boat with the rigging device with angle of attack of 0 degrees

3 The boat is put into the wind tunnel and the wind is activated

4 The drag force and lift force is measured using the Newton meters in the wind tunnel

5 Steps 2 to 4 are repeated 5 times and the mean of the forces is calculated

6 Steps 2 to 5 are repeated for angles of attack of 30, 60 and 90 degrees, as well as for each sail length of 5cm, 10cm and 15cm

Results + Discussion

Drag data

5cm	Reading (g)					Drag						
Angle(degrees)	**1**	**2**	**3**	**4**	**5**	**1**	**2**	**3**	**4**	**5**	**Average Drag**	**STDEV**
0	0	0	0	1	0	0	0	0	0.002243	0	0.00044857	0.000449
30	23	25	22	21	22	0.051585	0.056071	0.049343	0.0471	0.049343	0.050688	0.001521
60	40	43	37	36	42	0.089714	0.096442	0.082985	0.080742	0.094199	0.088817	0.003059
90	39	40	37	38	36	0.087471	0.089714	0.082985	0.085228	0.080742	0.085228	0.001586

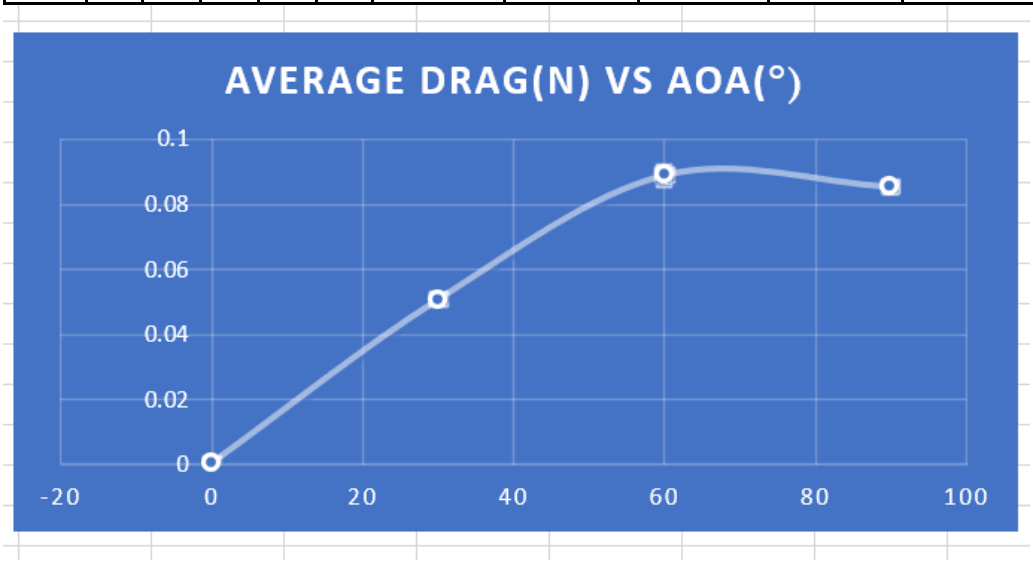

Figure 10.2.2: Drag Table + Graph, range 0 - 90, with error bars (5 cm sail)

10cm	Reading (g)					Drag						
Angle(degrees)	**1**	**2**	**3**	**4**	**5**	**1**	**2**	**3**	**4**	**5**	**Average Drag**	**STDEV**
0	0	0	2	1	0	0	0	0.004486	0.002243	0	0.0013457	0.000897
30	34	36	35	35	33	0.076257	0.080742	0.0785	0.0785	0.074014	0.077602	0.001144
60	47	56	58	57	63	0.105414	0.125599	0.130085	0.127842	0.141299	0.12605	0.005823
90	53	64	44	43	38	0.118871	0.143542	0.098685	0.096442	0.085228	0.10855	0.010293

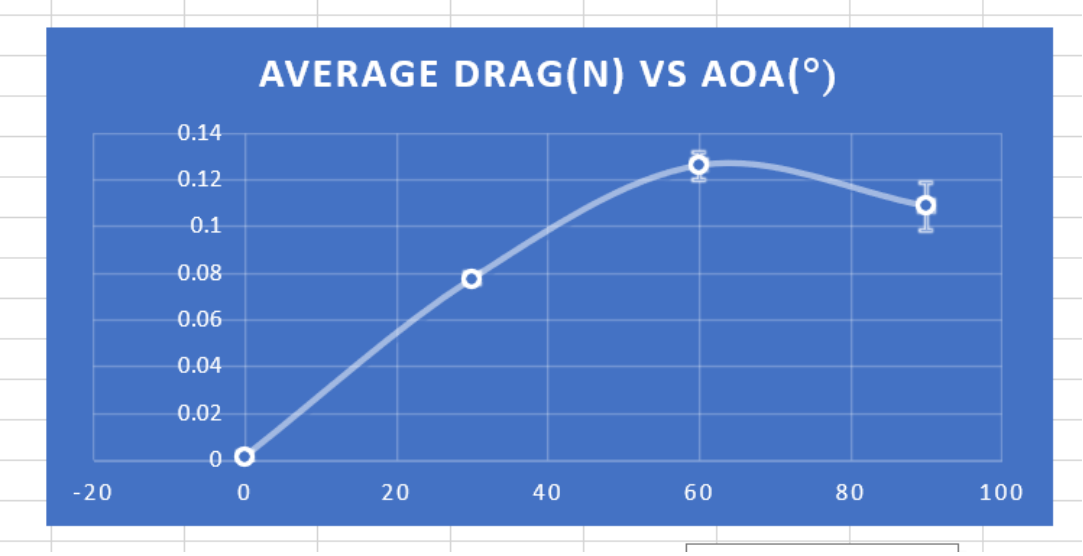

Figure 10.2.3: Drag Table + Graph, range 0 - 90, with error bars (10 cm sail)

15cm	Reading (g)					Drag						
Angle(degrees)	**1**	**2**	**3**	**4**	**5**	**1**	**2**	**3**	**4**	**5**	**Average Drag**	**STDEV**
0	0	3	5	0	2	0	0.006729	0.011214	0	0.004486	0.0044857	0.002128
30	38	33	35	34	43	0.085228	0.074014	0.0785	0.076257	0.096442	0.082088	0.00405
60	70	63	68	70	69	0.156999	0.141299	0.152513	0.156999	0.154756	0.152513	0.002924
90	72	48	83	74	86	0.161485	0.107656	0.186156	0.16597	0.192884	0.16283	0.015005

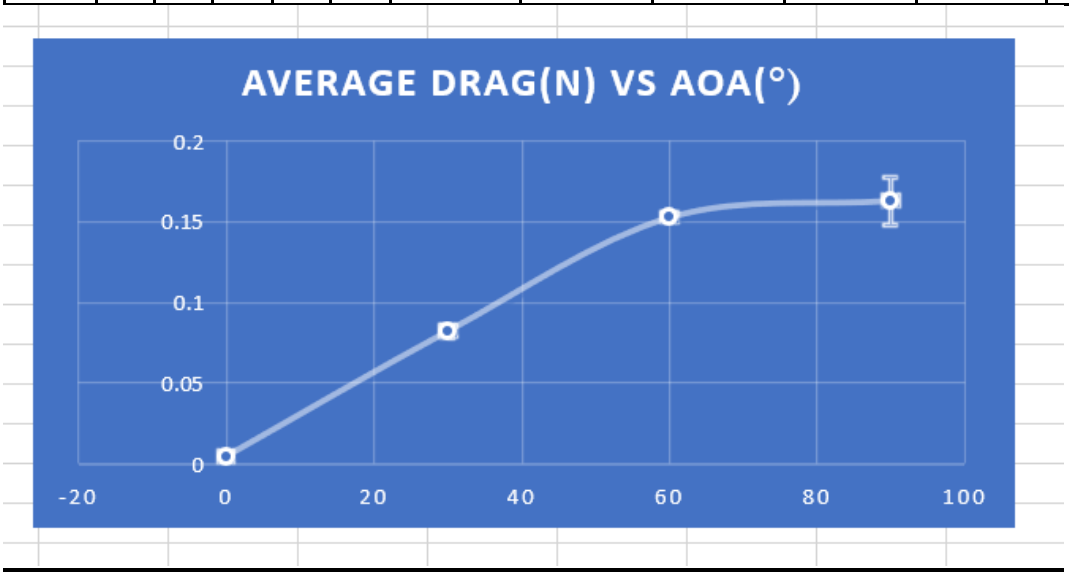

Figure 10.2.4: Drag Table + Graph, range 0 - 90, with error bars (15 cm)

Lift data

5cm	Reading (g)					Lift						
Angle(degrees)	**1**	**2**	**3**	**4**	**5**	**1**	**2**	**3**	**4**	**5**	**Average Drag**	**STDEV**
0	0	0	1	0	0	0	0	0.002243	0	0	0	0.000449
30	19	24	26	25	24	0.042614	0.053828	0.058314	0.056071	0.053828	30	0.052931
60	14	17	15	16	17	0.0314	0.038128	0.033643	0.035885	0.038128	60	0.035437
90	4	3	3	1	4	0.008971	0.006729	0.006729	0.002243	0.0089714	90	0.006729

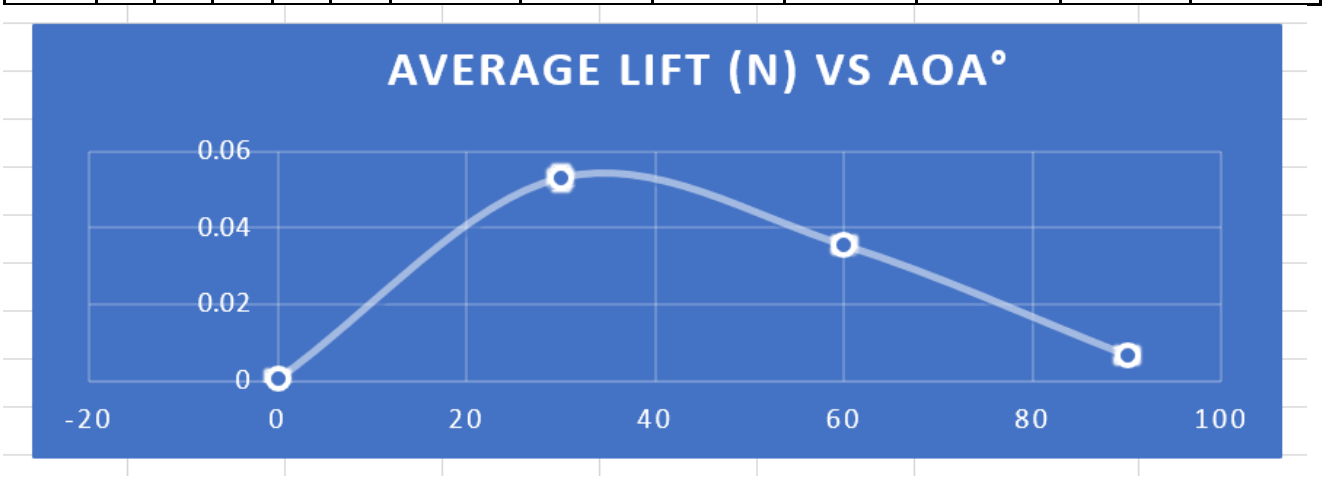

Figure 10.2.5: Drag Table + Graph, range 0 - 90, with error bars (5 cm sail)

10cm	Reading (g)					Lift						
Angle(degrees)	**1**	**2**	**3**	**4**	**5**	**1**	**2**	**3**	**4**	**5**	**Average Drag**	**STDEV**
0	0	2	1	0	0	0	0.004486	0.002243	0	0	0.001346	0.000897
30	25	26	30	27	25	0.056071	0.058314	0.067285	0.060557	0.056071	0.05966	0.00208
60	27	25	26	23	21	0.060557	0.056071	0.058314	0.051585	0.0471	0.054725	0.002416
90	0	0	0	0	0	0	0	0	0	0	0	0

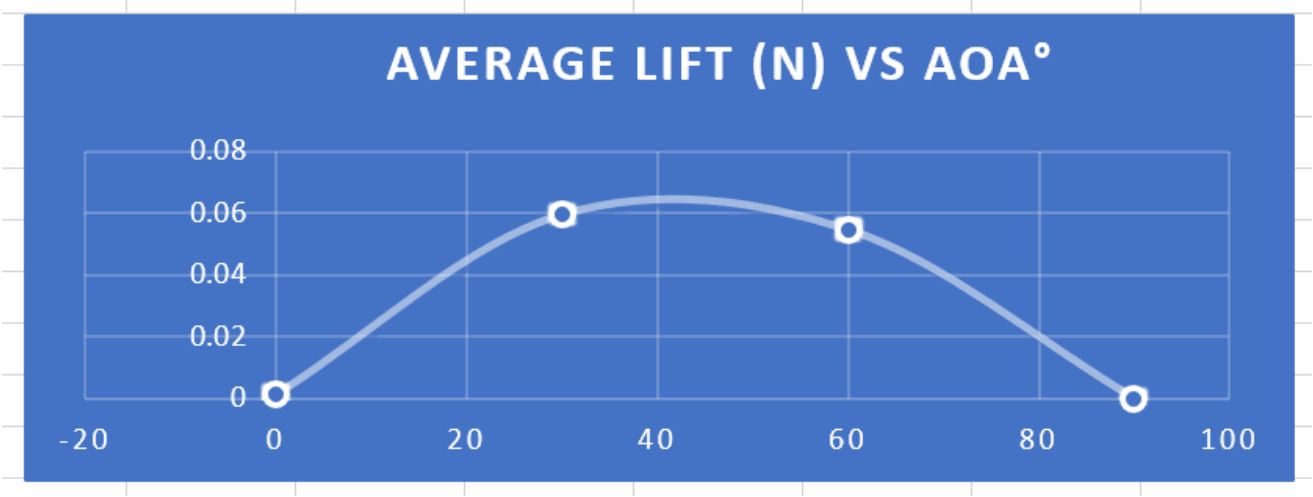

Figure 10.2.6: Drag Table + Graph, range 0 - 90, with error bars (10 cm sail)

15cm	Reading (g)					Lift						
Angle(degrees)	**1**	**2**	**3**	**4**	**5**	**1**	**2**	**3**	**4**	**5**	**Average Drag**	**STDEV**
0	2	2	1	0	0	0.004486	0.004486	0.002243	0	0	0.002243	0.001003
30	30	26	27	21	34	0.067285	0.058314	0.060557	0.0471	0.076257	0.061902	0.004842
60	21	20	26	24	25	0.0471	0.044857	0.058314	0.053828	0.056071	0.052034	0.002596
90	0	1	3	0	2	0	0.002243	0.006729	0	0.004486	0.002691	0.001308

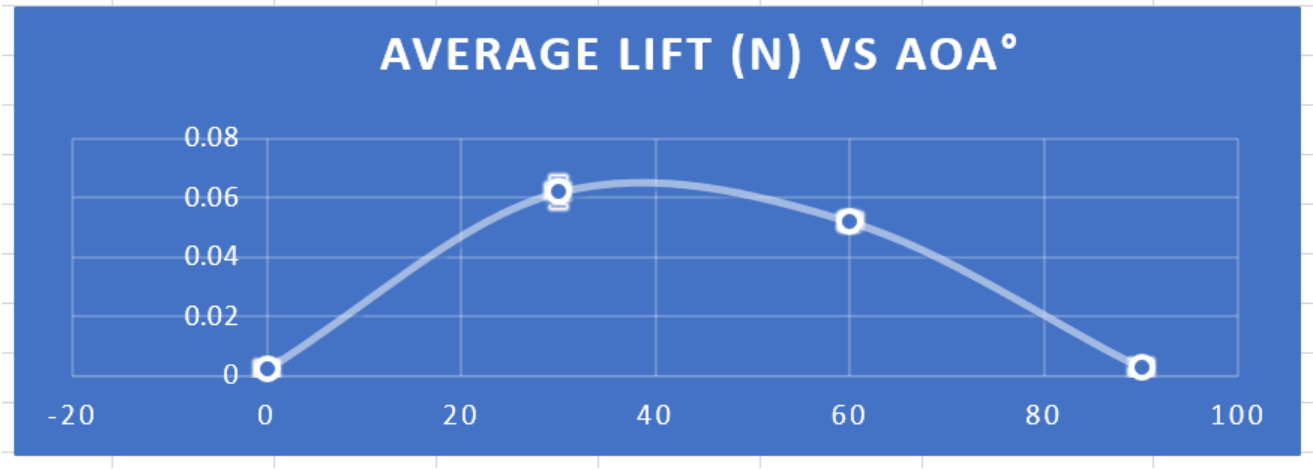

Figure 10.2.7: Drag Table + Graph, range 0 - 90, with error bars (15 cm sail)

For drag, the 15cm sail has the maximum drag achieved at 0.16283 N at a 90 degree angle of attack. For lift, the 10cm sail and 15cm sail have comparable maximum drag achieved at 0.05966

N and 0.061902 N at a 30 degree angle of attack respectively. Based on the measurement of lift and drag forces alone, the 15cm sail seems like the best option for the boat. However, on further testing with the rest of the optimised parts, it was found that the prototype capsized due to the lift force for the 15cm sail being too high. The 10cm sail had a better balance of lift and drag forces that prevented the boat from capsizing. Hence, the final prototype used the 10cm sail.

Possible Sources of Error Include:

Measurement error from cutting the sails

Only using the maximum average force achieved in our analysis

Conclusion

The 10cm sail is best suited for the design of the boat as it optimises both the drag and lift forces exerted on the boat such as to reduce the chance of capsizing.

10.3 Tan Yu Jay (Area of keel)

Aim of Experiment

To determine the best dimensions of a keel for our boat. We aim to strike a balance between stability and speed, such that the boat can complete the 30cm race as fast as possible while remaining upright.

Key Variables

Length of keel

Depth of keel

Area of keel (indirectly determined by above two variables)

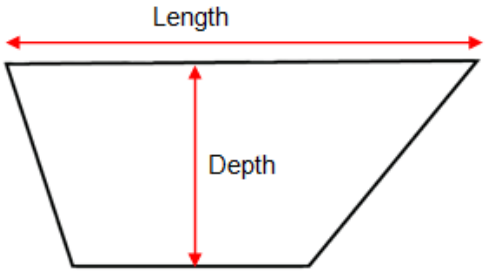

Constant Variables

- Force acting on the boat
- Distance travelled by boat
- Cross-sectional shape of keel

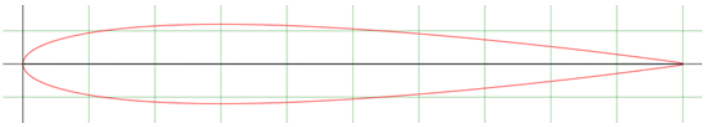

(We originally intended to use the NACA0008 airfoil shape for all the keel models, but had to switch to NACA0012, shown above, since the 3D printer was unable to print such a thin shape.)

By keeping the keel shape constant, we ensured an equal coefficient of drag across the different keels, thus allowing us to investigate only the area of the keel as we intended.

Apparatus

Boat

3D-printed keel models

Box of water

String and double-sided tape

Experimental Procedure

Below is our experimental setup.

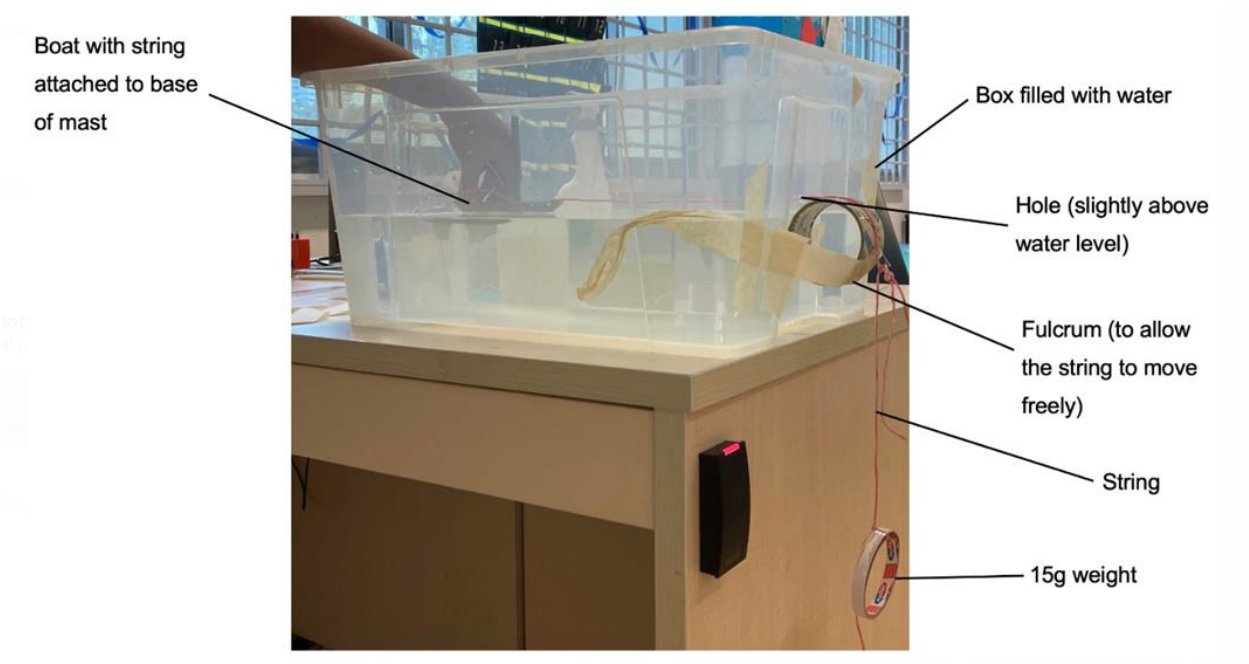

Figure 10.3.1 Experimental setup

1. This setup is explained in detail in Appendix B.
2. Place the boat at the far end of the box and release, allowing the weight to drag it across the water and travel the entire length of the box (50cm).
3. Use a camera to record this from the top. We used a 240fps camera. Below is a snapshot from one of the video clips.
4. Repeat this three times for each of the nine keels, for a total of 27 video clips.
5. Analyse the footage. By counting frames, determine the time taken for the boat to reach the other end of the box with different keels. Since the camera records at 240fps, we could record time intervals to a precision of 0.00417s.

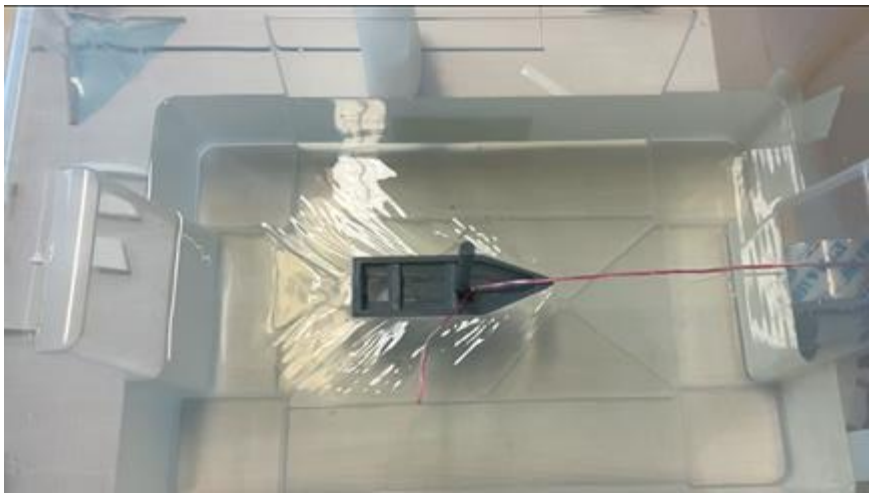

Figure 10.3.2: A frame from the video footage

Discussion of Results and Conclusion

Area of keel

The results we obtained were fairly indicative of a correlation between the area of the keel and the time taken for the boat to traverse the length of the box. Below is a table of the results. The average time was calculated using the simple formula **t = (trial1 + trial2 + trial3) / 720**, since the camera records at 240fps.

Length/cm	Depth/cm	Area/cm2	Trial 1 /frames	Trial 2 /frames	Trial 3 /frames	Average time/s
3	1	2.4	140	152	150	0.614
3	2	4.8	154	160	160	0.658
3	3	7.2	163	156	161	0.667
6	1	4.8	160	157	161	0.664
6	2	9.6	160	160	163	0.671
6	3	14.4	164	168	160	0.683
9	1	7.2	161	147	154	0.642
9	2	14.4	165	153	160	0.664
9	3	21.6	174	163	164	0.696

Table 10.3.1: Table of average times for various keel dimensions

Since we are only interested in how the area affects the speed of the boat, the data we need can be summarised in the graph below, which plots average time taken against area of the keel.

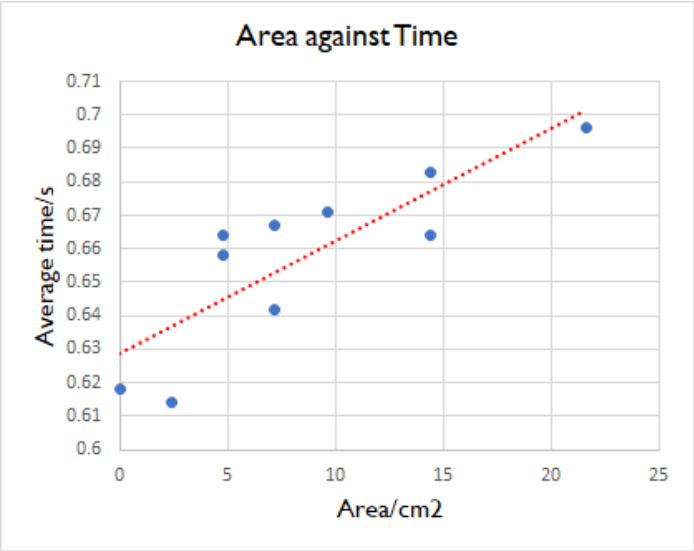

Figure 10.3.3: Graph of area of keels against time taken to travel the length of the tank

As can be seen from the trend line (red dotted line), the general relationship is that the greater the area of the keel, the faster the boat. This was our expected relationship, since the drag of a keel is directly proportional to its surface area:

$$F_{Drag} = \frac{1}{2} C_D \rho v^2 A$$

In addition, a larger keel would mean greater mass, which by Newton's Second Law directly impacts the acceleration of the boat.

It is interesting to note that the smallest keel (with an area of 2.4cm^2) yielded greater speed than without a keel at all (the data point where area = 0). Going by the above formula, a boat with no keel would theoretically travel faster than a boat with a small keel. However, this is clearly not the case. This result could be due to the fact that the bottom of the boat is very rough. In comparison, the keels are smooth and much more aerodynamically shaped than the random protrusions on the hull of the boat. Hence, adding even a small keel could greatly reduce the amount of turbulent flow caused by the rough hull, and create more laminar flow instead. Having less turbulent flow, the friction caused by the water drops correspondingly, and the boat can travel faster.

Stability of keel

Although we could not quantitatively measure this, a thorough analysis of the video footage revealed that larger keel areas corresponded to reduced turning about the boat's vertical axis. This is fairly straightforward, as the keel would present a greater reference area to the water (relative to direction of travel) when the boat is turned about its vertical axis. The larger reference area therefore produces a greater correcting moment to return the boat to its straight-line course. Furthermore, larger keels displayed greater resistance to tilting of the boat about its longitudinal

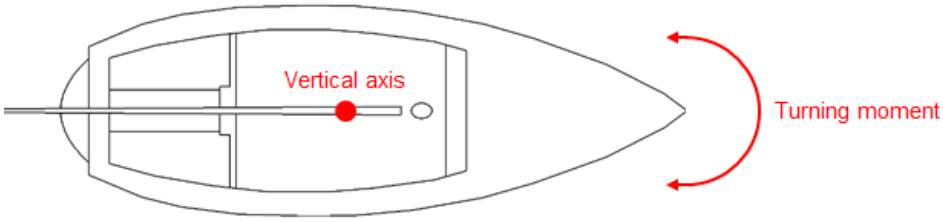

axis. Below is a simplified diagram showing the front view of a boat.

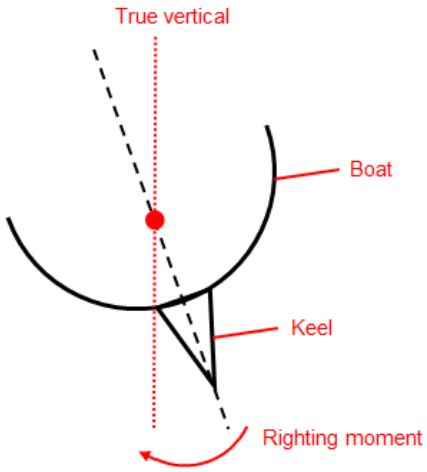

This result is also rather intuitive, since larger keels have greater mass. Therefore, they produce a greater righting moment, and can quickly correct any tilting of the boat about its longitudinal axis.

Conclusion

From these results, we can see that there must be a trade-off between stability and speed. Larger keels provide greater stability at the expense of lower speed. Since our goal is to design a boat which can travel 30cm in the shortest possible time, we initially decided to use the fastest keel available. From the graph, that would be the keel with area = 2.4cm^2 (length 3cm, depth 1cm). However, this keel did not provide reliable stability, and the boat fell over and sank numerous

during the testing. Hence, we ended up choosing the second smallest keel, with area = 4.8cm^2. There are two keels with area = 4.8cm^2, so we chose the better-performing keel (length = 3cm, depth = 2cm).

10.4 Lau Ian Kai, Ethan (Number and Arrangement of Keels)

Statement of Problem

To investigate how the number of keels and the arrangement of such keels (more specifically, the distance between keels) affects the time taken for the boat to travel a fixed distance of 50.0cm.

Variables

Independent variables: Number of keels, distance between keels

Dependent variable: Time taken for boat to travel 50.0cm

Constant variables: Initial velocity of boat, distance travelled by boat (50.0cm), type of keel (NACA 0012 hydrofoil), mass of weight pulling the boat, amount of water used.

Apparatus

3 NACA 0012 Airfoils (length 3.00cm, depth 2.00cm)

3D-Printed Boat

Box (filled halfway with water)

Camera (240 frames per second)

Double-Sided Tape

Fulcrum (roll of tape)

String

Tape

Weight (15g)

Procedure

1. Set up the apparatus as shown in Figures 9.9 and 9.10 (Appendix B), taking note that:
    a. The hole can be made using a soldering iron, and should be made slightly above the water level,
    b. The string should be able to slide freely along the fulcrum,
    c. The string should not be in contact with the water.
2. Using double-sided tape, attach one keel to the bottom of the sailboat, just under the mast.
3. Hold the sailboat at the end of the box away from the weight, with the back of the sailboat in contact with the box.
4. Using a camera which captures at 240 frames per second placed high above the set-up and capturing the entirety of the box to record a video, release the boat and allow the boat to be pulled to the other end of the box.

5. Using computer software, count the number of frames taken for the tip of the boat to come into contact with the other end of the box from release.
6. Convert the number of frames taken into the time taken for the boat to travel across the 50cm box, using the formula t=n/240, where n is the number of frames taken for the tip of the boat to come into contact with the other end of the box.
7. Repeat Steps 3-6 three times to obtain the mean time taken to travel 50cm, <t>.
8. Add a second keel behind the first, such that the distance between the back of the first keel and the front of the second keel d=0.00cm, and repeat Steps 3-7.
9. Repeat Step 8, changing the distance d between the keels each time.

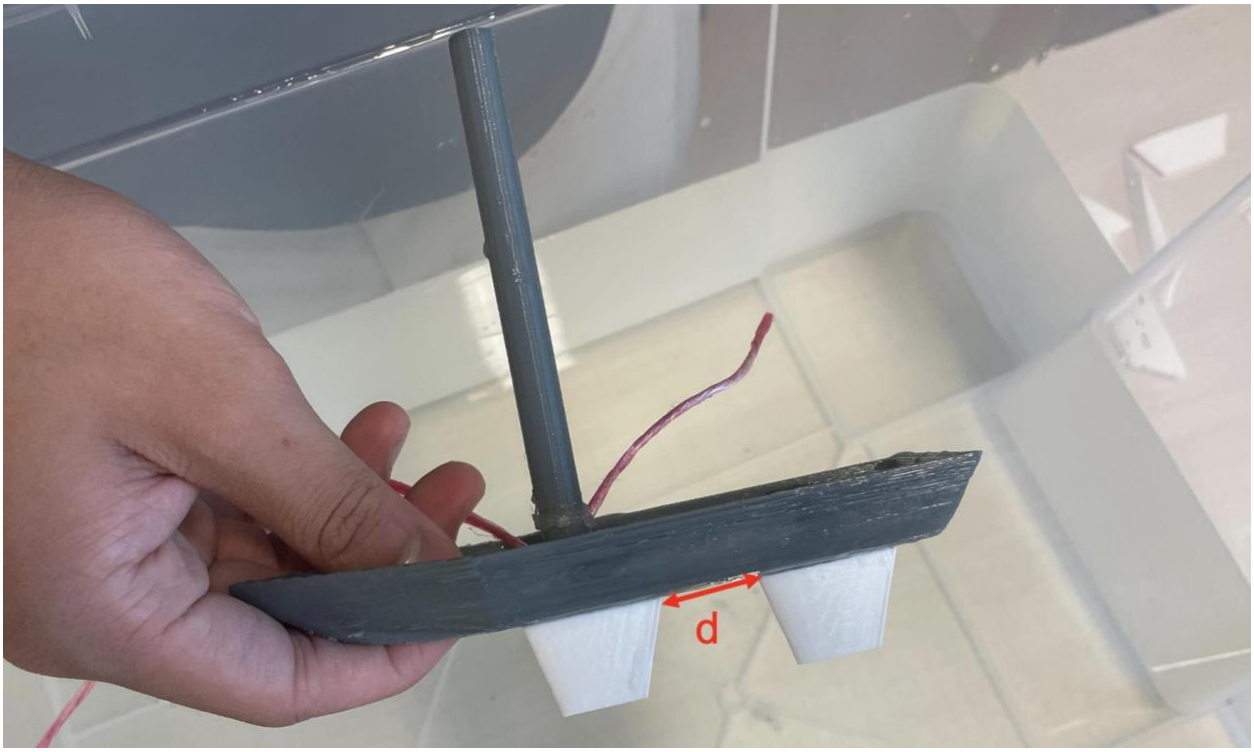

Figure 10.4.1: Image of the boat with multiple keels, separated by a distance d. The front of the boat is to the left.

Results and Conclusion

The table and graph below summarises the results that were obtained for varying numbers and arrangement of keels:

Number of Keels	Distance between keels /cm	Attempt 1		Attempt 2		Attempt 3		<t>/s
		Number of frames	Time/s	Number of frames	Time/s	Number of frames	Time/s	
1	N.A.	147	0.613	143	0.593	138	0.575	0.594
2	0.00	150	0.625	154	0.642	144	0.600	0.622
	0.20	160	0.667	155	0.646	157	0.654	0.656
	0.40	152	0.633	156	0.650	160	0.667	0.650
	0.60	150	0.625	152	0.633	149	0.621	0.629
	0.80	158	0.658	150	0.625	149	0.621	0.635
	1.00	147	0.613	149	0.621	148	0.617	0.617
	1.50	155	0.646	151	0.629	148	0.617	0.631
	2.00	155	0.646	142	0.592	155	0.646	0.628
3	N.A.	166	0.692	161	0.0.671	168	0.700	0.689

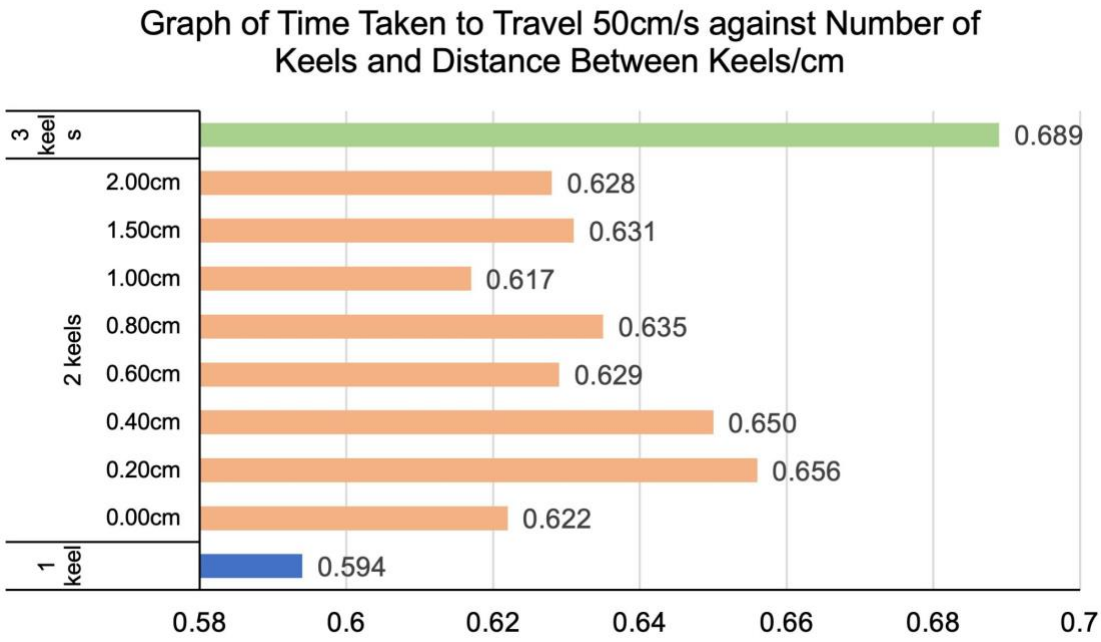

Figure 10.4.2: Table and graph of the relationship between number of keels, distance between keels and time taken to travel 50cm.

As can be seen from Figure 10.4.2, as the number of keels increases, the time taken for the boat to travel 50cm also increases. This is because when there are more keels, there is a greater friction drag due to the greater amount of area exposed to the water. Therefore, there will be more

drag. Hence, only one keel should be used for the final prototype, to ensure that the boat travels the fastest.

However, as the distance between the keels increases (for the 2 keeled set-up), we see an especially interesting result. From Figure 10.4.2, as the distance between keels increases from 0.60cm to 2.00cm, the time taken for the boat to travel 50cm remains relatively constant, at around 0.627s. Before remaining relatively constant at that value, however, there is a significant increase in the time taken at 0.20cm and 0.40cm, with times of 0.656s and 0.650s respectively. We hypothesise that this is the case, because as outlined in Section 3 and can be seen in Figure 10.4.3, the two boundary layers of the front keel recombine to form a wake at the end of the keel. This wake is highly turbulent. Hence, when the second keel meets this turbulence, it significantly increases the amount of drag experienced by the boat, causing it to slow down significantly (this is a 5.00% decrease in speed). However, between 0.40cm and 0.60cm, the wake has lost enough energy such that the water molecules of the wake have returned to laminar flow, causing the back keel to not have as much drag and hence take a shorter time to reach the endpoint.

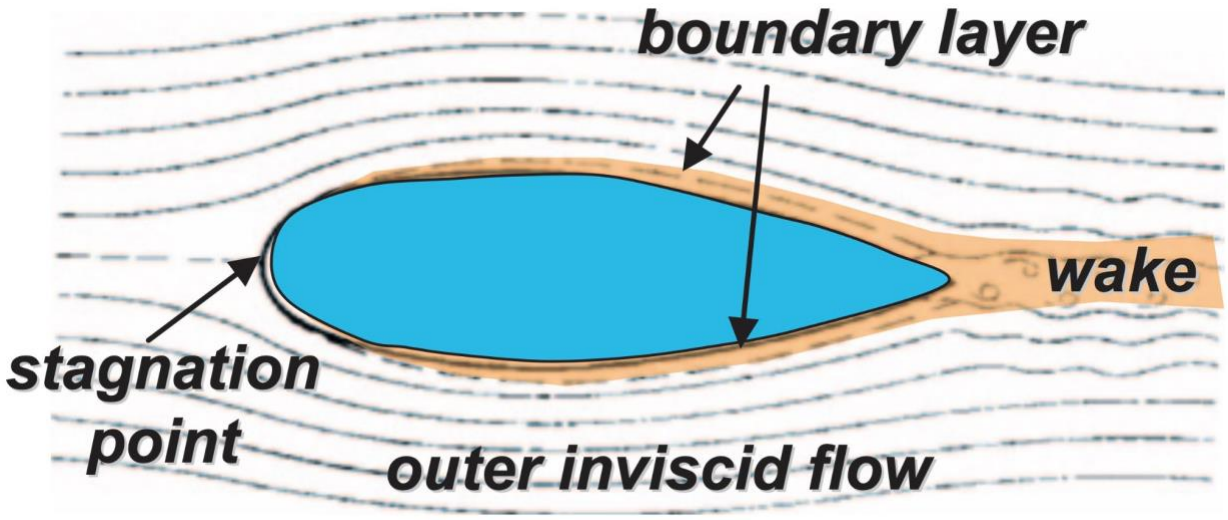

Figure 10.4.3 Layers of water around a hydrofoil (keel)

11 APPENDIX D: COMPUTATIONAL FLUID DYNAMICS

Whilst we are able to get empirical results and qualitatively explain why they work for both lift and drag values of the sail and keel, a quantitative model of these interfaces was not provided. This is as the problem of fluid flow has not been solved analytically. In fact, it is one of the 7 millennium problems in mathematics to prove that there exists an analytical solution to the Navier-Stokes' Equation in 3 Dimensions:

> Prove or give a counter-example of the following statement:
>
> In three space dimensions and time, given an initial velocity field, there exists a vector velocity and a scalar pressure field, which are both smooth and globally defined, that solve the Navier-Stokes equations.

As such, in order to gain any quantitative theoretical understanding into this problem, we have to turn to computational methods of fluid dynamics to model the fluid flow. All computational methods of fluid dynamics rely on making simplifying assumptions of the Navier Stokes' equations,

$$
\begin{aligned}
x: \quad & \rho\left(\frac{\partial u_x}{\partial t}+u_x\frac{\partial u_x}{\partial x}+u_y\frac{\partial u_x}{\partial y}+u_z\frac{\partial u_x}{\partial z}\right)=-\frac{\partial p}{\partial x}+\mu\left(\frac{\partial^2 u_x}{\partial x^2}+\frac{\partial^2 u_x}{\partial y^2}+\frac{\partial^2 u_x}{\partial z^2}\right)+\frac{1}{3}\mu\frac{\partial}{\partial x}\left(\frac{\partial u_x}{\partial x}+\frac{\partial u_y}{\partial y}+\frac{\partial u_z}{\partial z}\right)+\rho g_x \\
y: \quad & \rho\left(\frac{\partial u_y}{\partial t}+u_x\frac{\partial u_y}{\partial x}+u_y\frac{\partial u_y}{\partial y}+u_z\frac{\partial u_y}{\partial z}\right)=-\frac{\partial p}{\partial y}+\mu\left(\frac{\partial^2 u_y}{\partial x^2}+\frac{\partial^2 u_y}{\partial y^2}+\frac{\partial^2 u_y}{\partial z^2}\right)+\frac{1}{3}\mu\frac{\partial}{\partial y}\left(\frac{\partial u_x}{\partial x}+\frac{\partial u_y}{\partial y}+\frac{\partial u_z}{\partial z}\right)+\rho g_y \\
z: \quad & \rho\left(\frac{\partial u_z}{\partial t}+u_x\frac{\partial u_z}{\partial x}+u_y\frac{\partial u_z}{\partial y}+u_z\frac{\partial u_z}{\partial z}\right)=-\frac{\partial p}{\partial z}+\mu\left(\frac{\partial^2 u_z}{\partial x^2}+\frac{\partial^2 u_z}{\partial y^2}+\frac{\partial^2 u_z}{\partial z^2}\right)+\frac{1}{3}\mu\frac{\partial}{\partial z}\left(\frac{\partial u_x}{\partial x}+\frac{\partial u_y}{\partial y}+\frac{\partial u_z}{\partial z}\right)+\rho g_z.
\end{aligned}
$$

Figure 11.1: The Navier-Stokes equations

and then converging on approximations of solutions to these equations. Of these, a common approximation is an absence of viscosity, which leads to the Euler Equations

$$
\begin{cases}
\dfrac{\partial \rho}{\partial t}+\mathbf{u}\cdot\nabla\rho+\rho\nabla\cdot\mathbf{u}=0 \\
\dfrac{\partial \mathbf{u}}{\partial t}+\mathbf{u}\cdot\nabla\mathbf{u}+\dfrac{\nabla p}{\rho}=\mathbf{g} \\
\dfrac{\partial e}{\partial t}+\mathbf{u}\cdot\nabla e+\dfrac{p}{\rho}\nabla\cdot\mathbf{u}=0
\end{cases}
$$

Figure 11.2: The Euler equations

Through the software SimFlow, we were able to model the fluid dynamics of the keel. RANS modelling was used for turbulence under a k-epsilon model, as we want to take into account wake effects of the keel further away from its surface. The Navier Stokes equations were solved using a SIMPLE algorithm

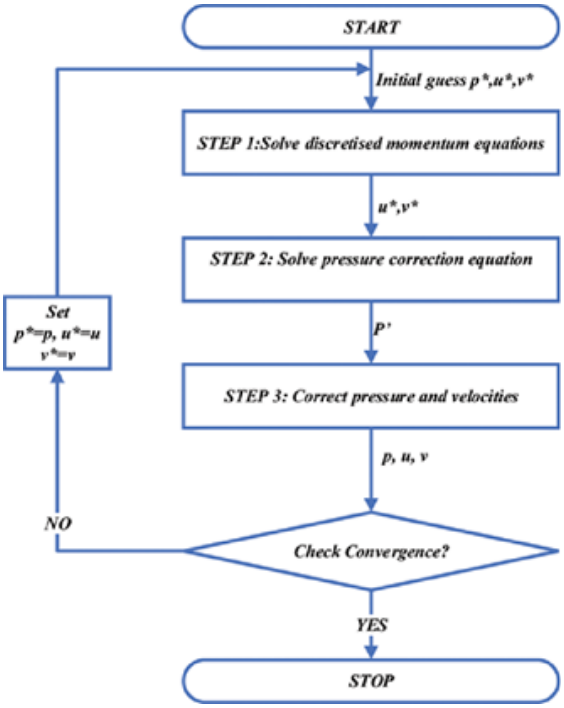

Fig. 11.3: SIMPLE Algorithm

Here are the results:

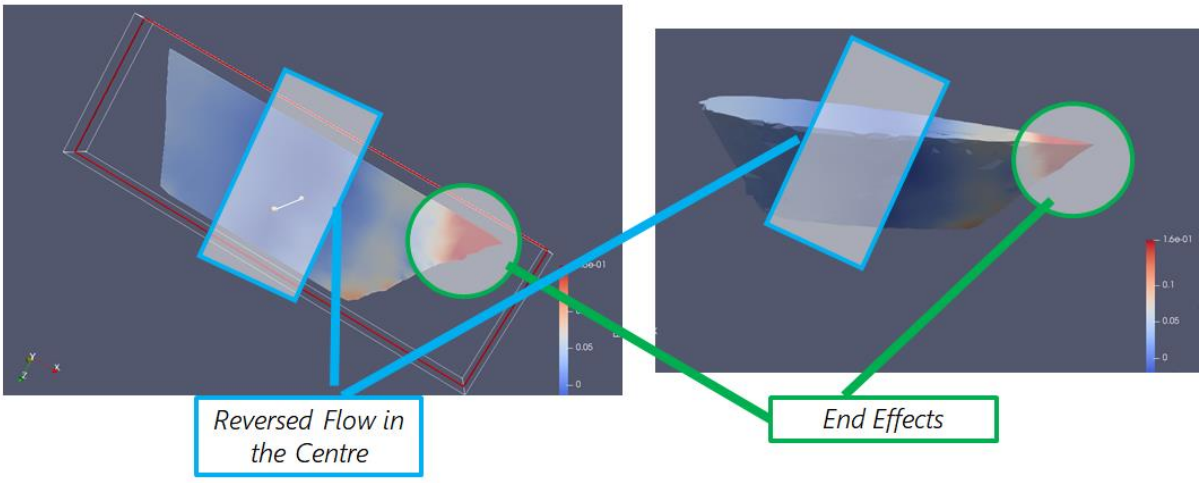

As you can see, we observe end effects with velocity increase at the tail end of the keel. Additionally, we observe a region of negative flow in the centre of the keel, where some vortex effects are being generated.

Unfortunately, modelling the sail is much more complicated. This is as the sail is a dynamic airfoil, and constantly changes its shape as wind is being blown onto it. Furthermore, the existing solvers

for airfoils, such as XFLR5 and Sail7 only work well for low angles of attack — at high angles of attack, they either fail to converge or produce questionable results, due to their handling of turbulence. Both these softwares extrapolate turbulence from Lift, which does not work well past the stalling point. A SimFlow model was also not possible, due to the difficulty of changing the AoA, and modelling a sufficiently realistic sail. Finally, physical flow visualisation using incense smoke was attempted, but was unfruitful as well. In the future, we hope to continue to work on and improve these methods, to get a nicer understanding of the flow of fluids around the sail. Whilst our theoretical understanding of how flow curvature caused a pressure differential was sufficient to the project, being able to understand how our airfoil geometries affected said flow curvature would have been useful as well, and may uncover some new insights into the design of the sail geometry.